^{3}H-Thymidine (^{3}H-TdR) incorporation analysis for assessment of cell proliferation

Cells were plated in a 96-well microplate (BD Biosciences, Billerica, MA, USA) at 2×10^5 cells per well in the presence or absence of GO containing 5, 10 or 100 ng/ml NAc-γ calicheamicin DMH or the respective concentration of hP67.6, in 100 μl of RPMI 1640 medium containing 10% fetal calf serum (FCS) and 1 μCi of ^{3}H-TdR. The detailed method was described in our previous papers.[3] The level of ^{3}H-TdR incorporation upon incubation with GO was compared with that upon incubation with hP67.6. The analysis was repeated five times.

Dye exclusion test with propidium iodide staining

After incubation of cells with GO or hP67.6. for the indicated period of time, cells were stained with 0.2 μg/ml propidium iodide (PI) (Sigma, Saint Louis, MO, USA) solution and counted. The numbers of dye-stained (dead) and unstained (living) cells both decreased and the amount of debris rapidly increased, making it difficult to evaluate the cell viability properly. Therefore, viable cells were evaluated. The viable cell count (/ml) after incubation with GO was compared with that after incubation with hP67.6. The analysis was repeated five times.

Cell cycle distributions

The cell cycle distribution was analyzed by flow cytometry with PI staining. The detailed method was described in our previous papers.[3,4] Cell cycle distribution could be analyzed after incubation with 10 or 100 ng/ml of GO for 24 or 48 h. GO temporarily arrests NB4 cells at the G2/M phase, and increases the percentage of hypodiploid cells, by which we evaluated the effect of GO.[3,4] Then, the GO-sensitive cells rapidly change to debris. The analysis was performed in triplicate.

Results

Flow cytometric analysis of CD33 and P-gp expression on NB4 cells and its sublines

The amount of CD33 expressed on the cells did not significantly differ among NB4, NB4/RA, NB4/MDR, NB4/RA/MDR and NB4/As cells. P-gp was not expressed on NB4, NB4/RA or NB4/As cells, in agreement with previous reports.[11,12] Equivalent levels of P-gp were expressed on NB4/MDR and NB4/RA/MDR cells.

^{3}H-TdR incorporation into NB4 cells and its sublines

Upon 72-h incubation with GO containing 5, 10 or 100 ng/ml of NAc-γ calicheamicin DMH, the level of ^{3}H-TdR incorporation into NB4 cells and its sublines decreased in a dose-dependent manner (Figure 1a). In each cell line, the level of ^{3}H-TdR incorporation was lower than that in the same cell line that had been incubated with the corresponding concentration of hP67.6. Upon incubation with GO containing 100 ng/ml NAc-γ calicheamicin DMH, there were significant differences in the level of ^{3}H-TdR incorporation between NB4 and NB4/MDR cells at 48 and 72 h ($P<0.01$ each), and between NB4/RA and NB4/RA/MDR cells at 48 and 72 h ($P<0.01$ each) (Figure 1b). There were no significant differences in the level of ^{3}H-TdR incorporation between NB4 and NB4/RA cells, or between NB4/MDR and NB4/RA/MDR cells at any time point. ^{3}H-TdR incorporation in NB4 cells upon 72-h incubation with GO containing 10 ng/ml NAc-γ calicheamicin DMH corresponded with that with 1000 ng/ml free NAc-γ calicheamicin DMH, which corresponded to a concentration of NAc-γ calicheamicin DMH that was approximately 100 times greater than that in GO. The rate did not change between P-gp-negative and positive NB4 cells.

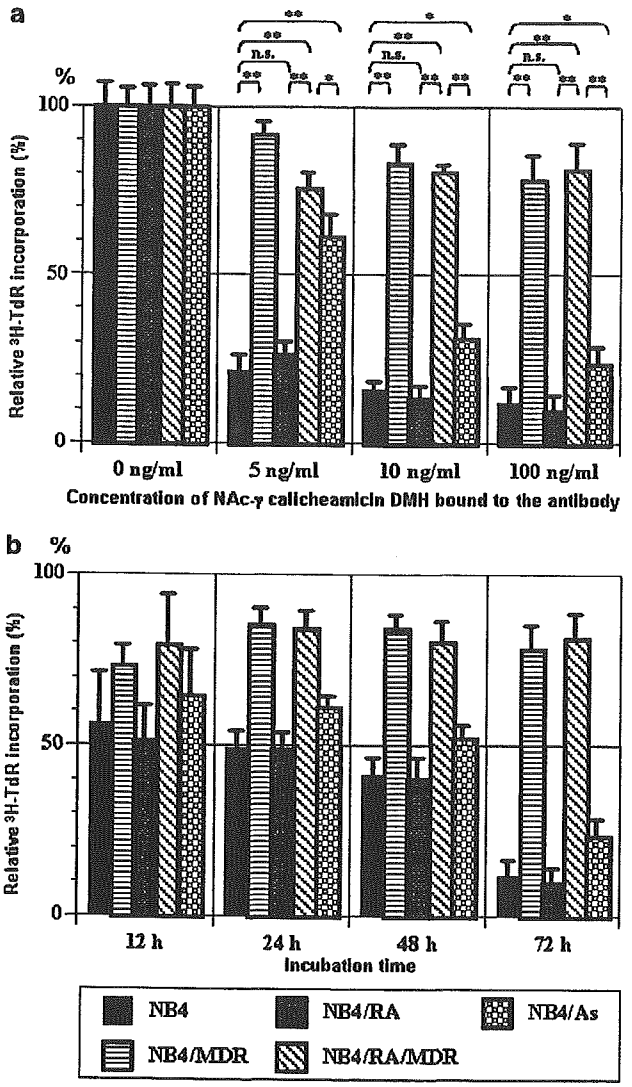

Figure 1 (a) ^{3}H-TdR incorporation by NB4 cells and its sublines after incubation with GO containing 5, 10 or 100 ng/ml NAc-γ calicheamicin DMH or with the respective concentrations of hP67.6 for 72 h. At 72 h, the amount of incorporated ^{3}H-TdR (cpm) was determined by liquid scintillation counting. In (a, b) the amount of incorporated ^{3}H-TdR are expressed as the ratio (%) of incorporated ^{3}H-TdR after incubation with GO to that after incubation with the respective concentration of hP67.6, normalized to 100%. The data from five independent experiments are expressed as mean values of the % response ± standard deviation (s.d.). At 72 h incubation with hP67.6, the mean level of ^{3}H-TdR incorporation by NB4 cells was 57 000 (53 200–62 300). Statistical significance was calculated by Student's *t*-test. $^*P<0.05$, $^{**}P<0.01$. (b) Time course of ^{3}H-TdR incorporation by NB4 cells and its sublines. Cells were incubated in medium with GO containing 100 ng/ml NAc-γ calicheamicin DMH or the respective concentration of hP67.6 for 12, 24, 48 or 72 h.

Viable cell count analysis by flow cytometry

By the incubation with GO containing 5, 10 or 100 ng/ml of NAc-γ calicheamicin DMH for 72 h, the viable cell counts of NB4 cells and its sublines decreased in a dose-dependent manner (Figure 2a). Figure 2c shows their cell counts upon 24-, 48- or 72-h incubation of these cell lines with GO containing 100 ng/ml NAc-γ calicheamicin DMH or the respective concentration of hP67.6. GO similarly decreased the number of NB4 and NB4/RA cells. GO also decreased the count of NB4/As cells. GO slightly reduced the counts of NB4/MDR and NB4/RA/MDR cells. The counts of NB4 cells and its sublines upon 72-h incubation with GO containing 10 ng/ml NAc-γ calicheamicin DMH corresponded with those with 1000 ng/ml free NAc-γ calicheamicin DMH, respectively.

The combination of ATRA and GO reduced the count of NB4 cells by a greater degree than GO or ATRA alone ($P=0.019$ and $P<0.01$, respectively), but did not reduce the count of NB4/RA cells by a significantly greater degree than GO or ATRA alone (Figure 2b). Upon incubation with GO and ATO, the counts of NB4 and NB4/RA cells were less than those upon incubation with GO ($P<0.01$ each) or ATO alone ($P<0.01$ each).

Cell cycle distribution

The increase percentage in the number of hypodiploid cells on cell cycle distribution upon incubation with GO containing 10 or 100 ng/ml of NAc-γ calicheamicin DMH for 48 h is summarized in Figure 3. The percentage of hypodiploid cells in the NB4, NB4/RA and NB4/As cells was increased upon 12-h incubation with GO, and it was the highest upon 48-h incubation. Beyond 48 h, it was difficult to evaluate the proportion of hypodiploid cells accurately because these GO-sensitive cells transformed into debris, as reported previously (Figure 4).[3] Upon incubation with GO, the percentage of hypodiploid cells in the NB4/MDR and NB4/RA/MDR cells were significantly less than those in the NB4 and NB4/RA cells, respectively ($P<0.01$ each). The addition of ATRA to GO further increased the percentage of hypodiploid cells in NB4 cells ($P=0.043$), but not in NB4/RA cells ($P=0.97$). Upon incubation with GO and ATO, the percentage of hypodiploid cells in NB4 and NB4/RA cells were slightly higher than those upon incubation with GO alone ($P=0.091$ and 0.082, respectively).

Similar results were obtained using blast cells derived from the patients with APL (Table 1). Upon incubation with GO for 48 or 60 h, the hypodiploid portion considerably increased in APL cells that had been obtained from not only the four cases at diagnosis, but also five ATRA-resistant and two ATRA- and ATO-resistant cases. Two patients, whose APL relapsed after achieving complete remission (CR) by ATRA and receiving postremission chemotherapy, were treated according to the Japanese phase 1 and 2 study of GO. They were resistant to re-induction therapy by ATRA, but achieved CR and CR without platelets recovery (CRp) after treatment with GO, respectively.

Discussion

Recently, GO with or without ATRA was introduced for the treatment of APL, and the clinical efficacy of these therapies has been reported in newly diagnosed or relapsed patients with APL.[6,7] There are two basic reasons that support the clinical

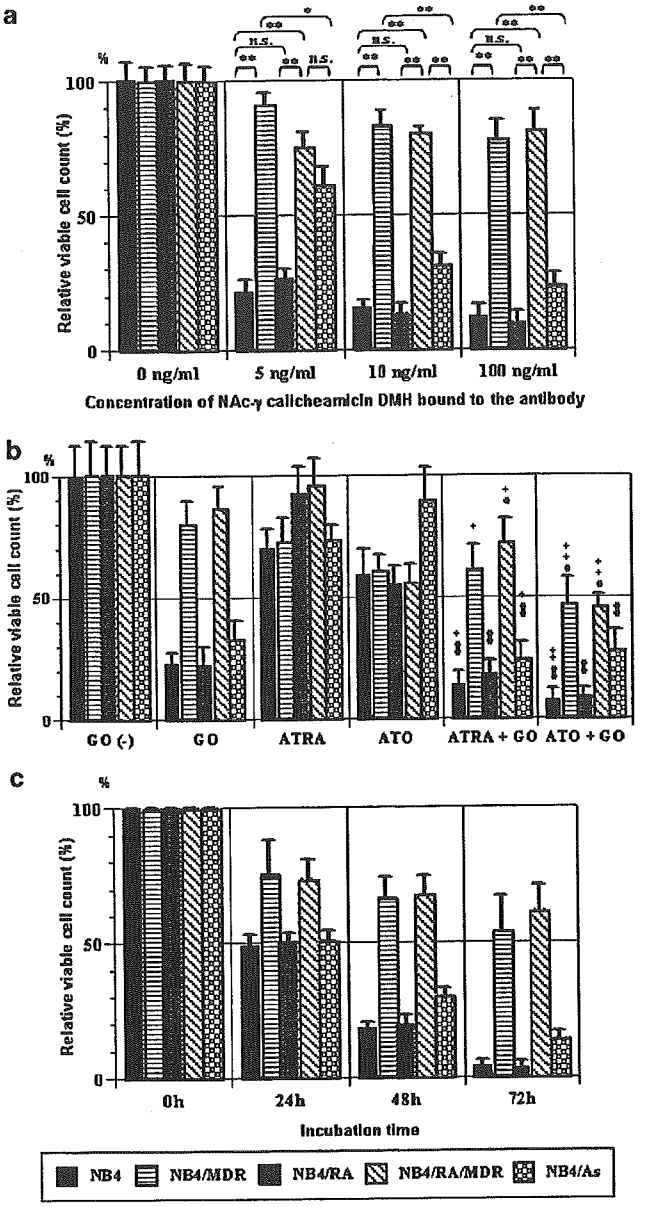

Figure 2 (a) Viable cell counts of NB4 cells and its sublines after incubation with GO containing 5, 10 or 100 ng/ml NAc-γ calicheamicin DMH or with the respective concentrations of hP67.6 for 72 h. The cell counts are expressed as the ratio of the cell counts after incubation with GO to that after incubation with the respective concentration of hP67.6, normalized to 100%. The data from five independent experiments are expressed as mean values of the % count±s.d. Statistical significance was calculated by Student's *t*-test. $^{*}P<0.05$, $^{**}P<0.01$. (b) Viable cell counts of the five cell lines upon incubation with GO containing 5 ng/ml NAc-γ calicheamicin DMH with or without ATRA or ATO for 72 h. The ratio of the cell count after incubation with the agents to that after incubation in the absence of both agents was calculated. Statistical significance was calculated by Student's *t*-test. $^{*}P<0.05$, $^{**}P<0.01$ comparing GO+ATRA or GO+ATO *vs* ATRA alone or ATO alone, respectively. $^{+}P<0.05$, $^{++}P<0.01$ comparing GO+ATRA or GO+ATO *vs* GO alone. (c) Viable cell counts of the five cell lines upon incubation with GO containing 100 ng/ml NAc-γ calicheamicin DMH, or with the respective concentration of hP67.6 for up to 72 h. The ratio (%) of the cell count after incubation with GO to that after incubation with the respective concentration of hP67.6 was calculated.

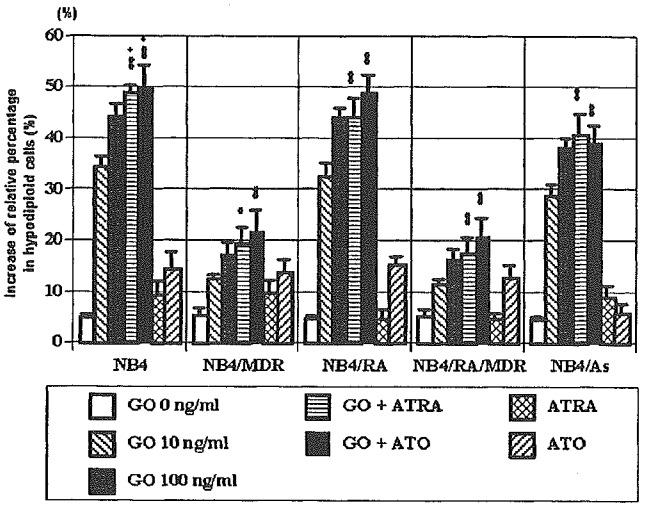

Figure 3 Percentage of hypodiploid cells in cell cycle distribution patterns upon 48-h incubation with GO containing 10 or 100 ng/ml of NAc-γ calicheamicin DMH or with the respective concentrations of hP67.6. Cells were also incubated with GO containing 100 ng/ml of NAc-γ calicheamicin DMH in combination with 10^{-6} M ATRA or 10^{-6} M ATO. Each bar represents the mean ± s.d. of three experiments. $^{*}P<0.05$, $^{**}P<0.01$ comparing GO + ATRA or GO + ATO *vs* ATRA alone or ATO alone, respectively. $^{+}P<0.05$, $^{++}P<0.01$ comparing GO + ATRA or GO + ATO *vs* GO alone.

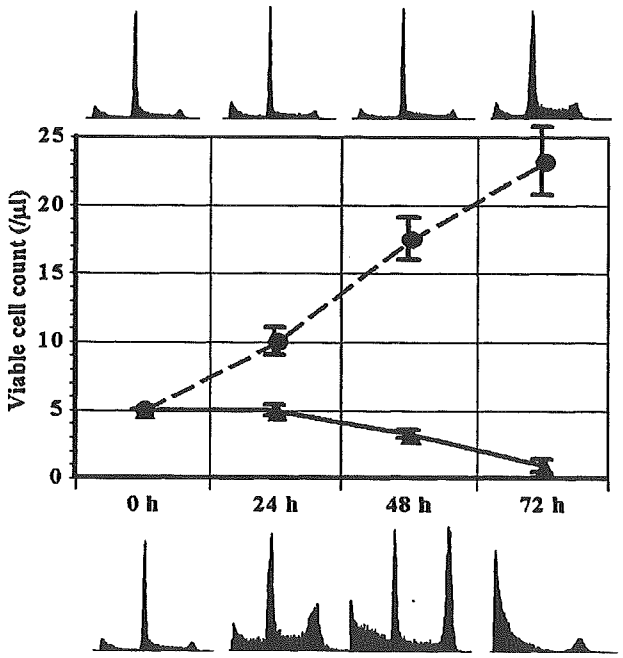

Figure 4 The cell growth curve and cell cycle distributions of NB4 cells upon 24-, 48- and 72-h incubation with GO containing 10 ng/ml NAc-γ calicheamicin DMH (continuous line and lower distribution patterns, respectively) or with the respective concentrations of hP67.6 (dotted line and upper distribution patterns, respectively).

application of GO on APL. One is that large amounts of CD33 are commonly expressed on the surface of APL cells. Therefore, several different anti-CD33 mAbs have been used for the treatment of APL, and notable results have been reported, especially in the use of GO.[6,7] Another reason is that a low level of P-gp is expressed on APL cells.[5] GO is sometimes not effective in some other subtypes of AML because the detached calicheamicin derivative is pumped out by P-gp.[3,4] Therefore, this mechanism of resistance to GO is not theoretically applicable to APL cells.

In this study, GO showed antiproliferative and cytocidal effects on ATRA-resistant NB4 cells as well as NB4 cells. We previously demonstrated that MDR modifiers, PSC833 and MS209, had no effect on ATRA-resistance in APL, which indicated that P-gp has a limited role in ATRA-resistance.[11] Intracellular ATRA concentration was not influenced by P-gp.[11] Clinical evidence, including our reports, also supported the independence of P-gp and ATRA-resistance.[13] Taking these data into consideration, GO is predictably effective on ATRA-resistant APL unless P-gp is expressed.

In the previous report, the combination of GO and ATRA was given to some patients with APL. In a study conducted in the US, GO was administered with ATRA to 19 patients with untreated APL.[6] The CR rate was 16/19 (84%), and 14 became PCR-negative. In relapsed APL, Lo-Coco *et al*[7] reported 14 cases of patients who achieved molecular remission after treatment with GO among 16 relapsed APL cases. However, there has been no *in vitro* study to explain these clinical efficacies. We performed the present study using NB4 and its drug-resistant sublines in an attempt to elucidate the mechanisms of GO. In APL, the drug resistance, which has been studied and discussed previously, might be built up by multiple causes and procedures.[8,13] Further studies on APL should be performed from many directions. It is also important to determine the optimal dosage of these drugs as well as the optimal timing of their administration.

GO also showed efficacy on ATO-resistant NB4 cells, which do not express P-gp. The cellular glutathione and MRP levels are reported with their relationship to ATO-resistance.[10,14] Walter *et al*[15] reported that MRP1 might attenuate the susceptibility to GO, although by a smaller degree than P-gp. We could not find an obvious relationship between MRP1 and GO-resistance.[16] Our data suggest that the MRP and the cellular glutathione levels play limited roles, while P-gp plays a major role in GO-resistance.

GO showed antiproliferative and cytocidal effects on APLs that do not express P-gp (Figure 4). GO increased the percentage of hypodiploid cells (Figure 3) while it inhibited cell proliferation in the early phase (Figures 1 and 2). After undergoing these changes, GO-sensitive cells rapidly collapsed into debris. The time-lag and variation of the effect of GO on APL cells might be explained by differences in the level of CD33 expression on the cells, and the length of time required for binding, and internalization of GO and detachment of calicheamicin from GO. Alternatively, GO could have various different actions against cells. Apoptosis, which is one of the main mechanisms of GO, did not explain all of the observed morphological changes of GO-treated cells in our previous study using videomicroscopy.[3] However, analysis of the changes in cell cycle distribution could be a valuable test for analyzing the susceptibility of AML cells to GO. It has a high degree of usability for samples derived from cases that contain different phenotypes.

We confirmed the antileukemia effect of GO on APL in an *in vitro* study using an APL cell line and its ATRA- and ATO-resistant sublines. GO seems to be promising for the treatment of not only untreated but also relapsed APL. A larger clinical study of GO for the treatment of relapsed and refractory APL is needed. The results of such study may suggest how GO should be integrated into the management of APL.

SPOTLIGHT

Table 1 Background of the patients and *in vitro* effect of GO on the cell cycle

Case no.	Sex	Age (year)	t(15;17)[a]	PML/RARα[b]	Status	Blast (%) in bone marrow	CD33 (%)	P-gp (%)	% increase in hypodiploid cells by GO[c]		Clinical response to ATRA	Clinical response to ATO	Clinical response to GO
									48 h	60 h			
DIAG-1	M	63	(+)	(+)	At diagnosis	92.2	99	3.7	13.2	22.7	CR	NT	NT
DIAG-2	F	21	(+)	(+)	At diagnosis	88.0	97.9	1.8	17.5	25.3	CR	NT	NT
DIAG-3	M	55	(+)	(+)	At diagnosis	67.6	97.8	3.5	12.1	17.9	CR	NT	NT
DIAG-4	M	51	(+)	(+)	At diagnosis	68.1	88.3	4.1	18.3	35.8	CR	NT	NT
ATRA-1	F	36	(+)	(+)	2nd relapse	20.2	98.7	1.8	10.7	18.4	NR	CR	NT
ATRA-2	M	57	(+)	(+)	2nd relapse	83.2	89.8	9.1	6.6	8.1	NR	CR	NT
ATRA-3	F	38	(+)	(+)	2nd relapse	77.2	94.6	1.4	16.9	27.9	NR	CR	NT
ATRA-4	F	21	(+)	(+)	2nd relapse	94.8	97.8	0.1	32.4	43.5	NR	CR	NT
ATRA-5	M	51	(−)	(+)	3rd relapse	30.8	97.9	4.4	9.6	12.8	NR	NT	CR
ATRA-6	M	48	(+)	(+)	3rd relapse	86.0	97.1	4.2	13.8	25.6	NR	NT	CRp
ATO-1	M	50	(+)	(+)	3rd relapse	78.0	83.6	11.6	10.8	13.4	NR	NR	NT
ATO-2	F	38	(+)	(+)	2nd relapse	38.7	85.4	4.5	9.5	15.3	NR	NR	NT

[a]Karyotype was analyzed by G-banding.
[b]PML/RARα was analyzed by RT-PCR or FISH.
[c]Defined as the difference in the percentage of hypodiploid cells between samples that had been incubated with nonconjugated anti-CD33 mAb or GO.
NT, not treated by ATO or GO *in vivo*; NR, no response; CR, complete remission; CRp, CR without platelets recovery.
After treatment with GO, the percentage of hypodiploid cells considerably increased in APL cells that had been obtained not only from the four patients at diagnosis but also from several ATRA-resistant patients and ATRA-and-ATO-resistant patients. Two patients, whose APL relapsed after achieving CR by ATRA and receiving postremission chemotherapy, were treated according to the Japanese phase 1 or 2 study of GO. They were resistant to reinduction therapy by ATRA, but achieved CR and CRp by treatment with GO, respectively. The coefficient of correlation (r) between the percentage of P-gp expression and the increase in hypodiploid portion was 0.60 and 0.65 upon 48- and 60-h incubation with GO, respectively.

Acknowledgements

We express our sincere gratitude to Ms Satoko Kanomi (Wyeth Pharmaceuticals Inc.) for continuous support, and to Ms Yoshimi Suzuki, Ms Noriko Anma and Dr Kiyoshi Shibata (Equipment Centre at Hamamatsu University School of Medicine) for technical assistance. This study was supported by Japanese grants-in-aid from the Ministry of Health and Welfare (No. 9-2) and the Ministry of Education and Science (No. 14570972).

References

1 Sievers EL, Larson RA, Stadtmauer EA, Estey E, Lowenberg B, Dombret H, *et al.*, Mylotarg Study Group. Efficacy and safety of gemtuzumab ozogamicin in patients with CD33-positive acute myeloid leukemia in first relapse. *J Clin Oncol* 2001; **19**: 3244–3254.
2 Linenberger ML, Hong T, Flowers D, Sievers EL, Gooley TA, Bennett JM *et al.* Multidrug-resistance phenotype and clinical responses to gemtuzumab ozogamicin. *Blood* 2001; **98**: 988–994.
3 Naito K, Takeshita A, Shigeno K, Nakamura S, Fujisawa S, Shinjo K *et al.* Calicheamicin-conjugated humanized anti-CD33 monoclonal antibody (gemtuzumab zogamicin, CMA-676) shows cytocidal effect on CD33-positive leukemia cell lines, but is inactive on P-glycoprotein-expressing sublines. *Leukemia* 2000; **14**: 1436–1443.
4 Matsui H, Takeshita A, Naito K, Shinjo K, Shigeno K, Maekawa M *et al.* Reduced effect of gemtuzumab ozogamicin (CMA-676) on P-glycoprotein and/or CD34-positive leukemia cells and its restoration by multidrug resistance modifiers. *Leukemia* 2002; **16**: 813–819.
5 Paietta E, Andersen J, Racevskis J, Gallagher R, Bennett J, Yunis J *et al.* Significantly lower P-glycoprotein expression in acute promyelocytic leukemia than in other types of acute myeloid leukemia: immunological, molecular and functional analyses. *Leukemia* 1994; **8**: 968–973.
6 Estey EH, Giles FJ, Beran M, O'Brien S, Pierce SA, Faderl SH *et al.* Experience with gemtuzumab ozogamycin ('mylotarg') and all-*trans* retinoic acid in untreated acute promyelocytic leukemia. *Blood* 2002; **99**: 4222–4224.
7 Lo-Coco F, Cimino G, Breccia M, Noguera NI, Diverio D, Finolezzi E *et al.* Gemtuzumab ozogamicin (Mylotarg) as a single agent for molecularly relapsed acute promyelocytic leukemia. *Blood* 2004; **104**: 1995–1999.
8 Gallaher RE. Retinoic acid resistance in acute promyelocytic leukemia. *Leukemia* 2002; **16**: 1940–1958.
9 Rybner C, Hillion J, Sahraoui T, Lanotte M, Botti J. All-*trans* retinoic acid down-regulates prion protein expression independently of granulocyte maturation. *Leukemia* 2002; **16**: 940–948.
10 Kitamura K, Minami Y, Yamamoto K, Akao Y, Kiyoi H, Saito H *et al.* Involvement of CD95-independent caspase 8 activation in arsenic trioxide-induced apoptosis. *Leukemia* 2000; **14**: 1743–1750.
11 Takeshita A, Shinjo K, Naito K, Ohnishi K, Sugimoto Y, Yamakawa Y *et al.* Role of P-glycoprotein in all-*trans* retinoic acid (ATRA)

resistance in acute promyelocytic leukaemia cells: analysis of intracellular concentration of ATRA. *Br J Haematol* 2000; **108**: 90–92.
12 Takeshita A, Shinjo K, Naito K, Matsui H, Shigeno K, Nakamura S *et al.* P-glycoprotein (P-gp) and multidrug resistance-associated protein 1 (MRP1) are induced by arsenic trioxide (As(2)O(3)), but are not the main mechanism of As(2)O(3)-resistance in acute promyelocytic leukemia cells. *Leukemia* 2003; **17**: 648–650.
13 Ohno R, Asou N, Ohnishi K. Treatment of acute promyelocytic leukemia: strategy toward further increase of cure rate. *Leukemia* 2003; **17**: 1454–1463.
14 Yang C-H, Kuo M-L, Chen J-C, Chen Y-C. Arsenic trioxide sensitivity is associated with low level of glutathione in cancer cells. *Br J Cancer* 1999; **81**: 796–799.
15 Walter RB, Raden BW, Hong TC, Flowers DA, Bernstein ID, Linenberger ML. Multidrug resistance protein attenuates gemtuzumab ozogamicin-induced cytotoxicity in acute myeloid leukemia cells. *Blood* 2003; **102**: 1466–1473.
16 Naito K, Takeshita A, Matsui H, Horii T, Maekawa M, Kitamura K *et al.* Multidrug resistance (MDR)-related protein 1 (MRP1) and lung resistance protein (LRP) are not the main drug resistance mechanisms of gemtuzumab ozogamicin (CMA-676) in AML. *Hematol J* 2002; **3**: 1048a.

SPOTLIGHT

Available online at www.sciencedirect.com
SCIENCE DIRECT
Biochimica et Biophysica Acta 1727 (2005) 125–133
BIOCHIMICA ET BIOPHYSICA ACTA BBA
http://www.elsevier.com/locate/bba

Transcriptional regulation of FKLF-2 (KLF13) gene in erythroid cells

Ayako Mitsuma[a], Haruhiko Asano[a,*], Tomohiro Kinoshita[a], Takashi Murate[b], Hidehiko Saito[a,1], George Stamatoyannopoulos[c], Tomoki Naoe[a]

[a]*Department of Hematology, Nagoya University Graduate School of Medicine, Tsurumai-cho 65, Showa-ku, Nagoya, 466-8550, Japan*
[b]*Nagoya University School of Health Sciences, Daiko-minami, 1-1-20, Higashi-ku, Nagoya, 461-8673, Japan*
[c]*Division of Medical Genetics, University of Washington, Seattle, WA, 98195-7720, USA*

Received 5 May 2004; received in revised form 15 December 2004; accepted 20 December 2004
Available online 6 January 2005

Abstract

FKLF-2 (KLF13) was cloned from fetal globin-expressing tissues and has been shown to be abundantly expressed in erythroid cells. In this study we examined the transcriptional regulation of the *KLF13* gene. A 5.5 kb 5′ flanking region cloned from mouse erythroleukemia (MEL) cell genomic DNA showed that major *cis* regulatory activities exist in the 550 bp sequence to the unique transcription start site, and that the promoter is more active in K562 cells than in COS-7 cells. The promoter was *trans*-activated by co-expressed GATA-1 through the sequence containing two CCAAT motifs, suggesting that GATA-1 is involved in the abundant expression of KLF13 mRNA in the erythroid tissue. Dual action, i.e. activating effect in COS-7 and repressive effect in K562 cell, was observed on its own promoter, suggesting a feedback mechanism for the transcriptional control of the KLF13 gene in the erythroid environment. These findings provide an insight on the mechanism of inducible mRNA expression of the *KLF13* gene in erythroid cells.

Keywords: Erythroid differentiation; KLF family; Promoter; Transcriptional regulation

1. Introduction

Proteins containing three contiguous Cys_2–His_2 zinc fingers similar to Sp1 or EKLF constitute a KLF family [1–3]. By using the zinc finger motif, these proteins bind to G-rich (GC or GT/CACCC) motifs that are widely distributed in *cis*-regulatory DNA sequences for gene expression. Some KLFs are ubiquitously expressed, while others show a tissue-restricted expression pattern. It may be reasonable to speculate that the non-ubiquitous KLFs are involved in cell type specific gene expression. Confirming this notion, EKLF (KLF1), which is specifically expressed in erythroid cells [4], plays a critical role for the expression of the β-globin gene [5,6] by interacting with the proximal CACCC motif of the β gene promoter [7,8]. LKLF (KLF2), which is predominantly expressed in the lung [9], is essential for the normal lung development since $LKLF^{-/-}$ ES cells do not contribute to the lung formation in chimeric mice [10]. KLFs thus play a substantial role in their major expression tissues.

Fetal *Krüppel*-like factor-2 (FKLF-2: KLF13) was originally cloned from mouse yolk sac and human fetal liver erythroid cells, i.e. fetal globin-expressing tissues [11]. It is predominantly expressed in the bone marrow, striated muscles and a subset of T cells. Other groups, in fact, cloned the same gene from these tissues [12,13]. Of note is that the mRNA expression of KLF13 gene is up-regulated upon the induction of differentiation with chemicals in cell lines with erythroid features [11]. Similarly, the expression of KLF13 protein is up-regulated upon the maturation of T cells [12]. These facts strongly suggest that KLF13 may be involved in the differentiation of the cells in which it is expressed. In addition KLF13 is a powerful activator of a broad range of promoters of erythroid genes in vitro [11]. These results suggest that

* Corresponding author. Tel.: +81 52 744 2158; fax: +81 52 744 2141.
E-mail address: asanoh@med.nagoya-u.ac.jp (H. Asano).
[1] Present address: Nagoya National Hospital, Sannomaru 4-1-1, Naka-ku, Nagoya 460-0001, Japan.

0167-4781/$ - see front matter © 2004 Elsevier B.V. All rights reserved.
doi:10.1016/j.bbaexp.2004.12.007

KLF13 plays a role in the development of erythroid phenotype. The transcriptional regulation for KLF13 gene expression may therefore be a part of molecular events of erythroid cell differentiation.

In this study we have cloned the 5′ flanking region of the mouse KLF13 gene. The promoter activity of the DNA fragment was tested in both erythroid (K562) and non-erythroid (COS-7) cells. Our data show that: the KLF13 gene promoter is more active in the erythroid environment than in the non-erythroid environment; and GATA-1 and KLF13 itself may have substantial effect in the transcriptional regulation of the KLF13 gene expression.

2. Materials and methods

2.1. Isolation of 5′ flanking DNA of the KLF13 gene

The 5′ flanking region of *KLF13* gene was obtained by inverse PCR (Fig. 1A). Four hundred nanograms of genomic

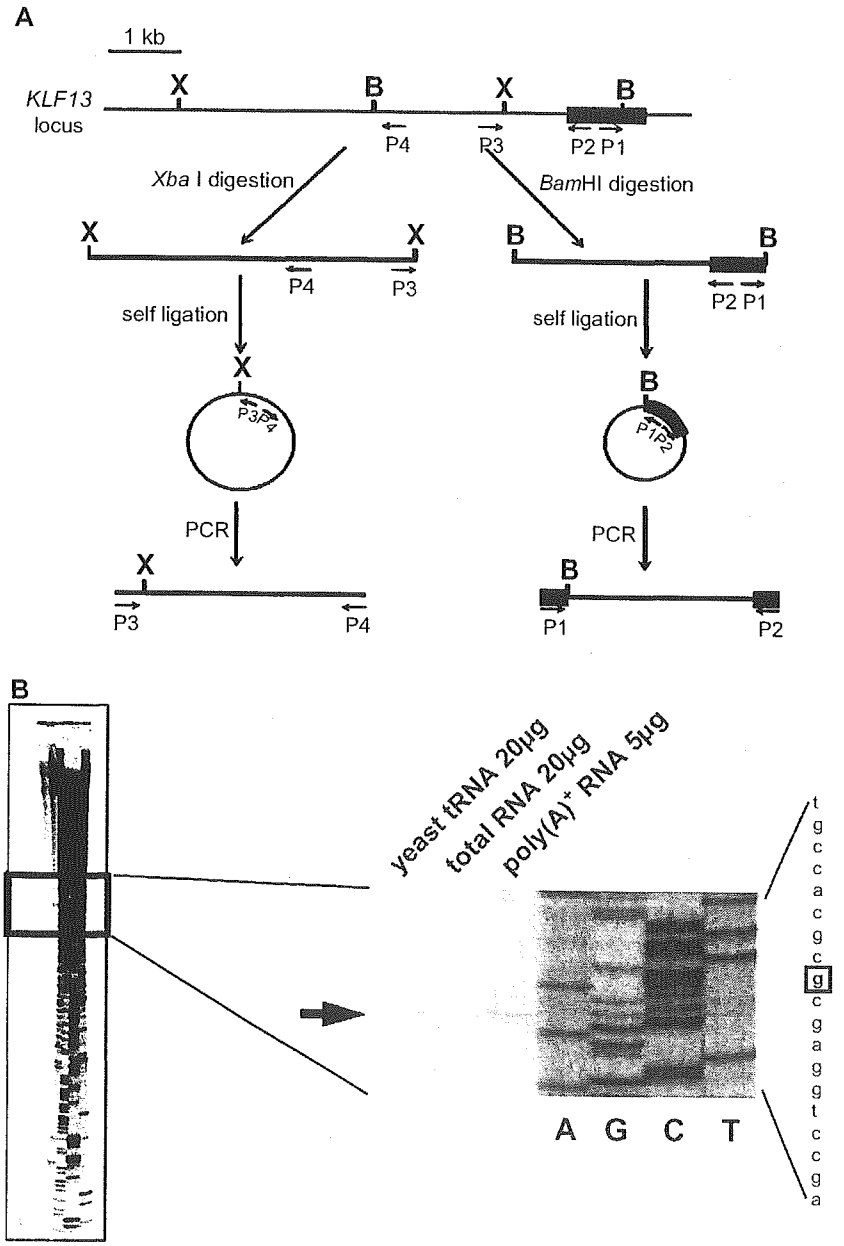

Fig. 1. Promoter of the *KLF13* gene. (A) Cloning of the 5′ flanking region of *KLF13* gene by inverse PCRs. The first exon is shown by a solid rectangle. B and X represent the *Bam*HI and *Xba*I sites, respectively. Primers used in inverse PCRs are indicated by arrows (P1–P4). Note that the positions of upstream *Bam*HI and *Xba*I sites are unknown prior to the experiments. (B) Primer extension analysis of KLF13 mRNA. RNAs used in the analysis are indicated above. Products of the sequencing reaction using the same probe were run on gel together, of which reading is shown at right. An arrow indicates the position of the extension product. The nucleotide in the sequence is highlighted by a square.

DNA extracted from MEL cells was digested with *Bam*HI or *Xba*I. Subsequently, the DNA was phenol-extracted, ethanol-precipitated and then self-ligated in 100 μL of reaction mixture at 16 °C for 30 min. The self-ligated DNA was dissolved in 8 μL low TE (5 mM Tris–HCl pH 8.0 and 0.1 mM EDTA) and 50 ng of the DNA was subjected to PCR by Expand Long PCR System (Roche) according to manufacture's instructions. The primer sets used in the PCR are 5′-GCCGCGACGGCAAGGACAGCC-3′ (P1) and 5′-GCATTGTGGCAGGCGGGACAGCC-3′ (P2), and 5′-GGTCTCCCTGACTTGATGGCTG-3′ (P3) and 5′-CAATGCTGAGGGAGTGAGCTAC-3′ (P4) for the *Bam*HI- and *Xba*I-cut DNA, respectively. The PCR products were cloned into T-vector (Promega) and were fully sequenced. The respective constructs were referred to pBam35 and pXba29.

2.2. Plasmid constructions

The 5.5 kb 5′ flanking DNA of the *KLF13* gene was reconstituted in pBluescript SK⁻vector (Stratagene). The *Not*I–*Bam*HI fragment from pBam35 was subcloned into the same sites of the vector (referred to pBS28). Subsequently, the *Bam*HI–*Xba*I (blunted) fragment of pXba29 was inserted at the *Bam*HI and *Eco*RV sites of pBS28 (referred to pBS55). The 5.5 kb DNA was cut as a *Not*I (blunted)–*Kpn*I fragment and inserted into pGL2-Basic vector (Promega) at the *Hin*dIII (blunted) and *Kpn*I sites (referred to pGL55). The truncation of the DNA was performed by either (1) blunting and self-ligation after double digestion with *Kpn*I and a desired enzyme or (2) cutting with *Xba*I and a desired enzyme (blunted), and subsequent re-insertion into the pGL2-Basic vector cut with *Sma*I/*Xba*I.

GATA-1 expression vector was constructed using the coding region of GATA-1 amplified by reverse transcription (RT)-PCR using random-hexamer-primed cDNA from MEL cell total RNA. The PCR primers are 5′-CAGGTTCAACCCCAGTGTTCCCA-3′ and 5′-CCTTCAAGAACTGAGTGGGGCG-3′. The cDNA fragment was cloned into the T vector, and correct amplification was verified by sequencing. Subsequently, the open reading frame was cut out as a *Sph*I (blunted)–*Sac*I fragment and subcloned into a eukaryotic expression vector pSG5DD [14] at the *Eco*RI (blunted) and *Sac*I sites.

Mutations were introduced using a kit (Altered Sites II in vitro Mutagenesis Systems, Promega) following the manufacture's instructions. The nucleotide substitution of individual motifs is listed in Table 1.

2.3. RNA extractions

Total RNA was extracted by a standard method [15]. Poly(A)$^+$ RNA was separated using an oligo (dT)-cellulose spun column (Pharmacia Biotech).

Table 1
List of nucleotide substitutions of *cis* elements

Motif	Sequence[a]	
	Wild type	Mutant
−0.37 kb CACCC	GGGTG	CTAGT
−0.23 kb CACCC	CACCC	ACTAG
Distal CCAAT	ATTGG	CAGAT
Proximal CCAAT	CCAAT	ATCTC

[a] Sense strand.

2.4. Primer extension and sequencing

Primer extension analysis was performed by a standard method [15]. An oligo DNA (5′-GCATTGTGGCAGGCGGGACAGCC-3′) was end-labeled with [γ^{33}P]ATP and 50,000 cpm was put into the extension reaction. Sequencing of the pBam35 by the same probe was performed using a kit (Cyclist, Stratagene).

2.5. Semi-quantitative RT-PCR

Semi-quantitative RT-PCR [11] was carried out using RQ1 DNase (Promega)-treated total RNA of COS-7 and K562 cells. The primers used for the amplification of KLF13 cDNA were 5′-TTCGCCTGCAGCTGGCAGGA-3′ and 5′-TGGCCGGGCTGATGGTGGG-3′. The condition of PCR was 95 °C (3 min) followed by variable number of cycles of 95 °C (30 s), 62 °C (30 s) and 72 °C (30 s).

2.6. Cell culture and transfections

K562 and COS-7 cells were cultured in RPMI1640 and DMEM, respectively, supplemented with 10% fetal calf serum. Transient transfections were performed using FuGENE 6 Reagent (Roche) according to the manufacture's instructions (reagent: DNA=3:1). Briefly, 1 μg plasmid DNA mixture (0.45 μg activator, 0.45 μg reporter and 0.1 μg pSVβ-Gal, or 0.9 μg reporter and 0.1 μg pSVβ-Gal) was transfected into 1×10^5 COS-7 and 5×10^5 K562 cells in 1 mL culture medium. COS-7 cells had been plated on a 12-well culture dish 24 h prior to the transfection. K562 cells were plated on the 12-well dish just before the transfection. After, the transfection cells were incubated at 37 °C for 24 h. Then, the cells were harvested, washed once with PBS and lysed in 200 μL Reporter Lysis Buffer (Promega). The cell lysate was subjected to luciferase and β-Gal assays as described elsewhere [8]. All transfections were performed three to five times in triplicate.

2.7. Data analysis and statistics

Data expressed as relative values to the average of the standard group were stored, analyzed and reported with the packages STATISTICA (StatSoft). Tukey's HSD (honestly significant difference) procedure (two-way ANOVA) was

used to evaluate the probability of significant differences. P values less than 0.05 were considered statistically significant.

3. Results

3.1. Promoter of the KLF13 gene

To examine the transcriptional regulation of *KLF13* gene, it was required to clone the 5′ -flanking DNA. When we started this project the DNA sequence was still uncovered. To determine the unknown genomic DNA sequence we carried out two sequential inverse PCRs using MEL cell genomic DNA (Fig. 1A). Each reaction gave rise to a single band (data not shown). Subsequently, these DNA fragments were fully sequenced, which revealed 6183 nucleotides. (GenBank accession no. AY601638). Using the DNA we first determined the transcription start site of the *KLF13* gene by the primer extension analysis. As illustrated in Fig. 1B the poly(A)$^+$ RNA generated a unique band that is at the nucleotide position 5471. A band at the same position, although faint, is formed from the total RNA while no bands were observed in the yeast tRNA. These results indicate that: the transcription of the KLF13 gene starts at a unique site, and the DNA obtained by inverse PCRs contains the promoter region of the KLF13 gene. The presence of the promoter activity was confirmed by the luciferase assay using K562 cells. The DNA fragment clearly raised the luciferase activity (pGL55 in Table 2). The average luciferase count driven by the KLF13 genomic DNA was about 314 times higher compared with that obtained from the control vector (pGL2-Basic). The same experiment was performed using COS-7, i.e. non-erythroid, cells. The pGL55 construct generated approximately 164-fold more luciferase counts compared with the pGL2-Basic vector (Table 2). The fold increase, i.e. 314 in K562 cells vs. 164 in COS-7 cells, was significantly different (P<0.001). These results show that: there exists a promoter activity in the DNA fragment that we cloned, and the promoter is more active in erythroid cells than in non-erythroid cells.

To test whether the different promoter activities were reflected to the gene expression, the expression of KLF13 mRNA was analyzed by semi-quantitative RT-PCR. Since the nucleotide sequence of the KLF13 gene of COS-7 cells was unknown, primers were set in the sequence common between mouse and human KLF13 cDNAs. The primer set amplified the COS-7 and K562 genomic DNA at a comparable efficiency (Fig. 2A). Subsequently, cDNAs of the two cell lines that were diluted to generate similar band patterns on amplification of 28S ribosomal RNA (rRNA) were subjected to PCR of the KLF13 gene. As shown in Fig. 2B cDNA of K562 cells yielded more intense bands in all cycles tested than that of COS-7 cells, demonstrating that higher expression of KLF13 mRNA in K562 cells than in COS-7 cells.

Table 2
Promoter activity of the 5.5 kb DNA fragment

	COS-7	K562
pGL2-Basic	1±0.17	1±0.23
pGL55	163.5±27.7	313.8±54.2

Luciferase counts were corrected by the β-Gal activities. The average luciferase activities obtained from pGL2-Basic vector was considered as 1. Data are expressed as mean±1 S.D. of three independent transfections in triplicate.

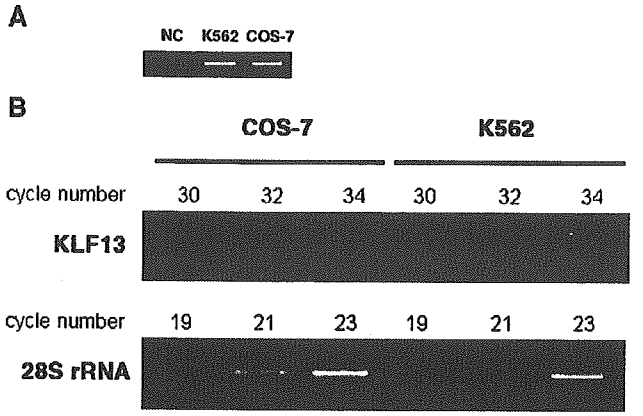

Fig. 2. Expression of KLF13 mRNAs in COS-7 and K562 cells. (A) PCR using the same amount of genomic DNA. One hundred nanograms of genomic DNA was amplified by 33 cycles of PCR in a 50 μL reaction volume. Subsequently, 10 μL was run on gel. Note that similar bands were generated in COS-7 and K562 cells, indicating comparable efficiencies of amplification between the two cell lines. NC means negative control in which TE buffer instead of DNA was put in the PCR reaction. (B) Semi-quantitative RT-PCR using COS-7 and K562 cell cDNAs. The numbers shown above indicate PCR cycles. Note the similar amplification of 28S rRNA gene between the two cells, and obviously more intense bands on the amplification of KLF13 gene in K562 cells than in COS-7 cells.

3.2. Erythroid cell specific regulation of the KLF13 gene promoter

To elucidate the *cis* regulatory elements of the KLF13 gene promoter, a series of truncated DNA fragments were prepared (Fig. 3A) and their promoter activities were analyzed in COS-7 and K562 cells. Results are expressed as promoter activities relative to those obtained from the 0.13 kb DNA fragment (considered as 1). As shown in Fig. 3B, in COS-7 cells promoter activities were significantly different between 5.5 and 2.9 kb (P<0.001), 2.0 and 0.73 kb (P<0.001), 0.55 and 0.37 kb (P<0.001), 0.37 and 0.29 kb (P<0.001), 0.29 and 0.22 kb (P<0.001), and 0.22 and 0.13 kb (P<0.001), suggesting that two DNA regions, i.e. −0.13 to −0.37 kb and −0.73 to −2.0 kb, function as positive regulatory elements while −0.37 to −0.55 kb and −2.9 to 5.5 kb DNA regions function as negative regulatory elements in non-erythroid cells (Fig. 3C). Since the 0.37 kb fragment exhibited the most powerful promoter activity, which is 12.4-fold higher relative to that of 0.13 kb fragment, among the 9 truncated promoters, major

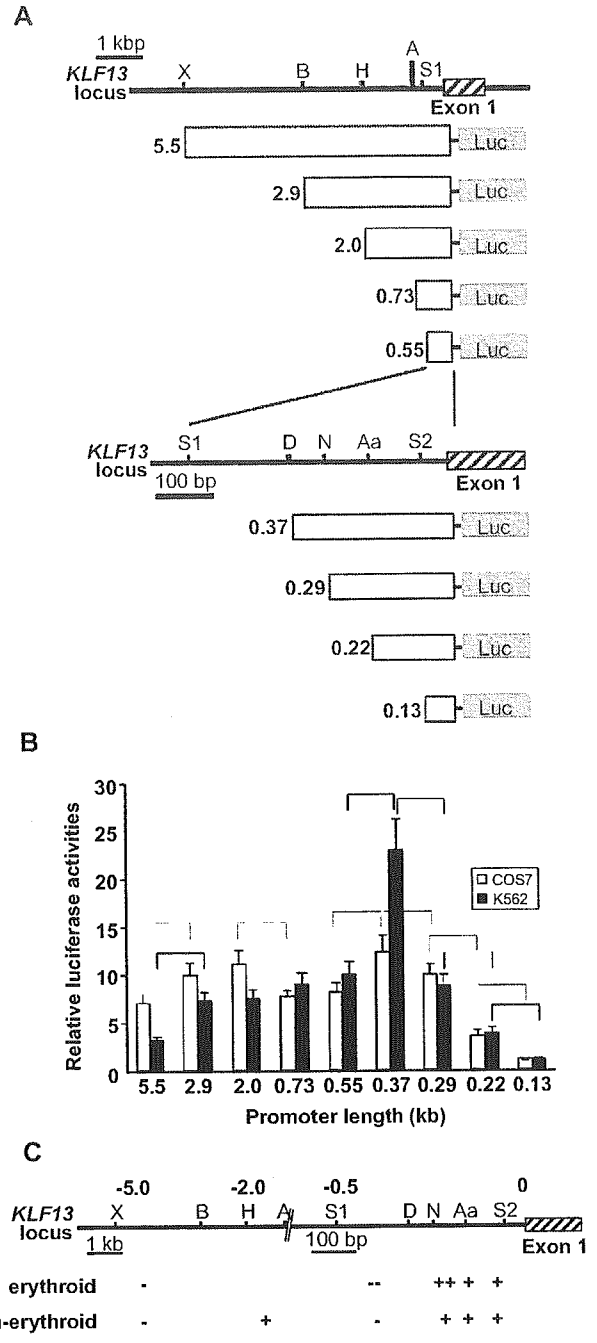

Fig. 3. Activities of KLF13 gene promoter in erythroid and non-erythroid cells. (A) Reporter constructs and *KLF13* locus. Luciferase gene is driven by truncated promoters indicated by light gray rectangles. Restriction sites used for the truncation are indicated above. Abbreviations for restriction sites are X, *Xba*I; B, *Bam*HI; H, *Hin*dIII; A, *Apa*I; S1, *Sac*I; D, *Dra*III; N, *Nae*I; Aa, *Aat*II; and S2, *Sac*II. The length of the promoters is shown at left in kb. (B) Relative luciferase activities obtained from COS-7 (gray bars) and K562 (black bars) cells are shown. Luciferase counts were corrected by the β-Gal activity, and the average count obtained from the 0.13 kb promoter was considered as 1. Error bars indicate one S.D. Results were obtained from three independent transfections in triplicate. Promoter pairs showing significantly different activities are indicated by broken (COS-7) and solid (K562) lines. (C) Positive (+) and negative (−) regulatory regions of KLF13 gene promoter. *KLF13* locus is shown above and numbers are the distance to the transcription start site in kb. Note that the scale is altered at 0.7 kb position. Regions having a potent effect are indicated by ++ and − −.

promoter activities exist in this DNA sequence. The highest promoter activity of the 0.37 kb fragment was also observed in K562 cells (Fig. 3B). However, it is of note that the activity is 22.9-fold higher than that of the 0.13 kb fragment, which should be contrasted to the 12.4-fold increase observed in COS-7 cells. The relative promoter activities of DNA fragments containing the upstream sequence (5.5, 2.9 and 2.0 kb) were not as high as those of COS-7 cells (Fig. 3B). The relative activities of 0.73 and 2.0 kb promoters were 9.0 and 7.5, respectively, which was not statistically significant (P=0.46). Therefore the positive regulatory effect of the −0.73 to −2.0 kb region observed in COS-7 cells was absent in K562 cells (Fig. 3C). Together, it is suggested that: the 80 bp sequence between −0.29 and −0.37 kb is more powerful in an erythroid environment than in a non-erythroid environment (expressed as ++ in Fig. 3C), and among the negative regulatory elements the −0.37 to −0.55 kb sequence has a strong effect (expressed as - in Fig. 3C) since the powerful activity of the −0.29 to −0.37 kb region disappeared in the presence of the 180 bp, i.e. −0.37 to −0.55 kb, DNA.

3.3. The erythroid factor GATA-1 and KLF13 are potential transcriptional regulators of the KLF13 gene promoter

The results shown above indicate that: the regulation of KLF13 gene promoter is distinct in erythroid cells, and major regulatory elements of the promoter are located in the proximal 550 bp region. Inspection and computer database search (TRANSFAC, http://www.motif.genome.jp/) of the DNA sequence revealed a number of transcription factor binding sites. Of remark is the presence of multiple GC, CACCC and GATA-1-binding motifs (Fig. 4), suggesting that Sp1/KLF and GATA factors participate in the regulation of KLF13 gene promoter. To test how the transcription of *KLF13* gene is regulated in erythroid cells we analyzed the effects of GATA-1 and KLF13, both of which are expressed in erythroid cells, on the KLF13 gene promoter. The expression vectors of these factors and luciferase reporter constructs were co-transfected into COS-7 and K562 cells. To focus the *cis* sequence corresponding to the effects, if any, of these factors we utilized three promoters with different length, i.e. 0.55, 0.29 and 0.13 kb fragments. As shown in Fig. 5A GATA-1 activated the 0.55 and 0.29, but not 0.13, kb promoters in COS-7 cells. The respective fold increases compared with

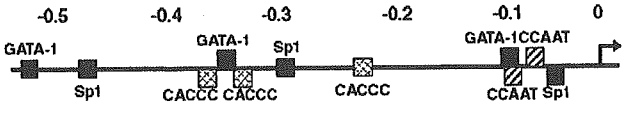

Fig. 4. *cis* elements of the 0.55 kb promoter that are potentially recognized by Sp1/KLFs and GATA-1. Numbers shown above are the distance to the transcription start site in kb. Motifs are indicated by black (GATA-1), gray (Sp1), hatched (CACCC) and striped (CCAAT) squares. The transcription start site is indicated by an arrow.

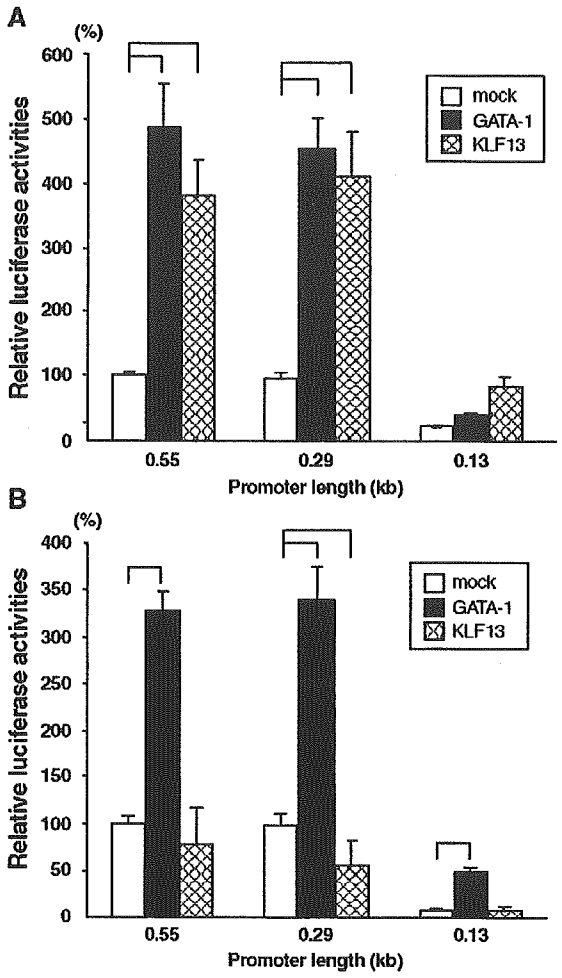

Fig. 5. (A and B) Effects of GATA-1 and KLF13 itself on the KLF13 gene promoter. Relative luciferase activities derived from 0.55, 0.29 and 0.13 kb promoters are shown. Reporter constructs were co-transfected with either mock, GATA-1 or KLF13 into COS-7 (A) and K562 (B) cells. Luciferase counts were corrected by the β-Gal activity, and the average count of the 0.55 kb promoter obtained from mock-transfected cells was considered as 100%. Error bars indicate one S.D. Solid lines shown above indicate that the promoter activities were significantly different. Results were obtained from three (COS-7) and four (K562) independent transfections in triplicate.

its absence were 4.9 (P<0.001), 4.7 (P<0.01) and 1.9 (P=0.99). The activation of the KLF13 gene promoter by GATA-1 was also observed in K562 cells (Fig. 5B). In the presence of GATA-1 the respective promoter activities were 3.3, 3.5 and 6.5 times higher compared with those without GATA-1 (P<0.001 in all promoters). These results show that GATA-1 is a potential *trans*-activator of the KLF13 gene promoter, and the proximal 130 bp DNA sequence is capable of mediating the GATA-1 effects specifically in the erythroid environment. In addition it is noteworthy that the 0.55 and 0.29 kb promoters showed essentially the same activities, which is similar than the result shown in Fig. 3B, in any experimental condition, suggesting that neither GATA-1 nor KLF13 is responsible for the erythroid specificity in the sequence between −0.55 and −0.29 kb (Figs. 3B and C).

KLF13 activates its own promoter in COS-7 cells (Fig. 5A). The activities of the 0.55, 0.29 and 0.13 kb promoters in the presence of KLF13 were 3.8 (P<0.01), 4.2 (P<0.01) and 4.0 (P=0.05) times higher compared with its absence. In K562 cells, however, this was not the case — i.e. the respective promoter activities relative to those mock-transfected were 0.78 (P=0.27), 0.56 (P<0.001) and 1.04 (P=1.0) (Fig. 5B). KLF13 thus failed to activate its own promoter in K562 cells. Rather, KLF13 tended to repress the 0.55 and 0.29 kb promoters.

3.4. GATA-1 activates KLF13 gene promoter through the sequence containing CCAAT motifs

The data shown above indicate that erythroid specific GATA-1-responsive element(s) of the KLF13 promoter are present in the very proximal 0.13 kb sequence. There is a non-canonical GATA-1-binding site within the sequence (Fig. 4). In addition two CCAAT boxes could be a potential GATA-1-binding site [16,17]. We, however, failed to demonstrate GATA-1-binding to these sequences by gel shift experiments, in which there was a distinct GATA-1-binding to the canonical GATA sequence (data not shown). Therefore, we focused on the role of activation by GATA-1 of the major *cis* elements in the 0.13 kb sequence, i.e. two CCAAT boxes. Mutations were introduced into individual CCAAT motifs of the 0.55 kb KLF13 gene promoter. We analyzed how these mutations affect the activity of GATA-1 on the promoter in K562 cells by transient transfection experiments. Results are shown in percentage luciferase counts relative to that obtained from mock-transfected wild type (WT) promoter (considered as 100%). As illustrated in Fig. 6 mutation of the single CCAAT motifs failed to affect the basal promoter activity: 83% in $CCAAT^{mut1}$ (P=0.73), and 105% in $CCAAT^{mut2}$ (P=1.0). In contrast to these single mutations, double mutation ($CCAAT^{mut3}$) brought about remarkable decline of the promoter activity (15%, P<0.001). GATA-1 activated these CCAAT-mutated promoters, however the relative luciferase activities were significantly lower in $CCAAT^{mut1}$ (185%, P<0.001), $CCAAT^{mut2}$ (303%, P<0.001) and $CCAAT^{mut3}$ (56%, P<0.001) compared with that of WT (406%). Thus GATA-1 less effectively activated CCAAT-mutated KLF13 gene promoters.

3.5. KLF13 represses its own promoter in K562 cells

As shown in Fig. 5B KLF13 has a tendency to repress its own promoter in K562 cells. Since this was observed in 0.55 and 0.29 kb promoters, and not in 0.13 kb promoter, we focused on two CACCC motifs located at the −0.37 and −0.23 kb positions, potential target sequences of the KLF13 protein. Mutations were introduced into individual motifs of the 0.55 kb promoter ($CACCC^{mut1}$, $CACCC^{mut2}$ and $CACCC^{mut3}$ in Fig. 7). We tested whether the mutations affect the suppressive activity of KLF13 on its

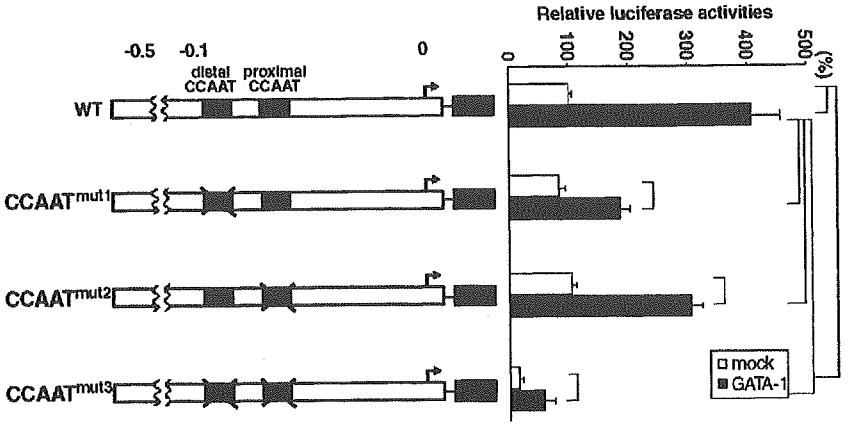

Fig. 6. Role of CCAAT motifs for the activity of GATA-1 on the KLF13 gene promoter. They were disrupted by point mutations listed in Table 1. Promoters lacking the distal, proximal and both CCAAT motifs are referred to $CCAAT^{mut1}$, $CCAAT^{mut2}$ and $CCAAT^{mut3}$, respectively, which are shown in the left panel. The numbers shown above are the distance to the transcription start site in kb. The right panel shows the relative luciferase activities tested in K562 cells. Luciferase counts were corrected by the β-Gal activity, and the average count of wild type (WT) promoter without co-expressed GATA-1 was considered as 100%. Error bars indicate one S.D. Solid lines shown at the right indicate that the promoter activities were significantly different. Results were obtained from three independent transfections in triplicate.

own promoter in K562 cells by the transient transfection assay. Results are shown in percentage luciferase counts of the basal WT promoter (Fig. 7). Mutations did not reduce the promoter strength at all: 119% for $CACCC^{mut1}$ (P=0.61), 111% for $CACCC^{mut2}$ (P=0.96) and 102% for $CACCC^{mut3}$ (P=1.0). In the presence of KLF13 the average luciferase counts were low: 78% (WT), 85% ($CACCC^{mut1}$), 82% ($CACCC^{mut2}$) and 57% ($CACCC^{mut3}$). The respective fold increases from the basal promoter activity were 0.78 (P=0.46), 0.71 (P=0.03), 0.74 (P=0.11) and 0.56 (P=0.001). It was thus consistently observed that KLF13, to some extent, represses its own promoter. The repressive effect was strengthened by the mutations of the two CACCC boxes.

4. Discussion

KLF13 gene is highly expressed in erythroid cells, and its mRNA expression is up-regulated upon the induction of differentiation in erythroid lines [11], which raises the possibility that KLF13 participates in molecular events of erythroid cell differentiation. In view of this it is of interest to investigate how the transcription of the KLF13 gene is regulated in erythroid cells. In this study we cloned and characterized the 5′ flanking regulatory region of the KLF13 gene.

We identified a unique transcription start point of KLF13 gene. To reveal how the transcription is regulated in erythroid cells we analyzed the promoter activity of the

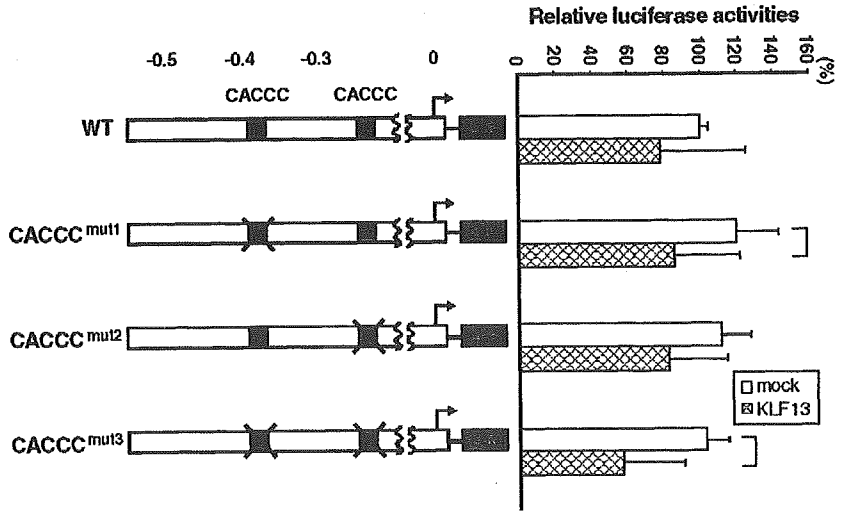

Fig. 7. Role of CACCC motifs for the activity of KLF13 on its own promoter. They were disrupted by the point mutations listed in Table 1. Promoters lacking the −0.37 kb, −0.23 kb and both CACCC motifs are referred to $CACCC^{mut1}$, $CACCCT^{mut2}$ and $CACCC^{mut3}$, respectively, which are shown in the left panel. The numbers shown above are the distance to the transcription start site in kb. Right panel shows relative luciferase activities tested in K562 cells. Luciferase counts were corrected by the β-Gal activity, and the average count of wild type (WT) promoter without co-expressed KLF13 was considered as 100%. Error bars indicate one S.D. The solid lines shown at the right indicate that the promoter activities were significantly different. Results were obtained from five independent transfections in triplicate.

5.5 kb flanking DNA sequence in K562 and COS-7 cells. Our data show that the KLF13 gene promoter in the erythroid environment is more powerful than in the non-erythroid environment, which may be related to the higher KLF13 gene expression in K562 cells than in COS-7 cells (Fig. 2B). In addition positive and negative regulatory regions were at least in part different between the two environments. Of particular interest is the DNA sequence with a potent positive activity between −0.29 and −0.37 kb, which was distinctive in erythroid cells. However, the potent promoter activity disappeared when the −0.55 kb DNA was used, which in turn suggests the presence of a potent negative regulatory activity in the DNA sequence between −0.37 and −0.55 kb. The identification of *cis* elements responsible for the positive and negative regulation of these DNA sequences may be the next step to uncover the mechanism of erythroid cell specific transcriptional control of the KLF13 gene.

It is interesting that the KLF13 gene promoter was activated by KLF13 itself in COS-7 cells, whereas this was not the case in K562 cells. Rather, the promoter tended to be repressed in the presence of KLF13, suggesting that there exists a feedback mechanism in the control of KLF13 gene transcription in erythroid cells. *cis* Element(s) responsible for the repressive action of KLF13 remain to be elucidated. Regarding this issue we explored the role of two CACCC boxes of the KLF13 gene promoter. Mutations of the two CACCC motifs, however, made the repressive effect of KLF13 more evident. This might be relevant to the fact that these CACCC motifs were likely involved in the *trans*-activation of the promoter by KLF13 itself in COS-7 cells since KLF13 failed to sufficiently activate the promoter (data not shown). Therefore, it is suggested that the CACCC boxes may be key *cis* elements corresponding to the *trans*-activating effect of KLF13 on its own promoter.

We have shown that the KLF13 promoter is *trans*-activated by GATA-1, indicating that KLF13 is potentially a downstream gene of GATA-1. The mechanism by which GATA-1 activates the KLF13 gene promoter needs to be determined. The fact that the promoter with distal CCAAT box mutation was less effectively activated by GATA-1 ($CCAAT^{mut1}$ in Fig. 6) should be taken into account, which suggests that the distal CCAAT box or the overlapping non-canonical GATA-1-binding site may play a role in the KLF13 promoter activation by GATA-1. This may be supported by the observation that the reduction of the activation of the $CCAAT^{mut1}$ by GATA-1 was significant, $P<0.01$, when the same experiment was performed using COS-7 (data not shown). The overlapping CCAAT box and GATA-1-binding site of the KLF13 promoter is structurally similar to the Aγ globin gene promoter [16]. In contrast to the Aγ promoter where GATA-1 binding could be demonstrated by gel shift assays, we have failed to demonstrate GATA-1 binding to the KLF13 promoter containing CCAAT motifs. How does GATA-1 activate the KLF13 promoter in such a situation? There are two possibilities: either GATA-1 binds to the promoter region but the binding is too weak to be detected; or the activation of the promoter by GATA-1 is indirect, a case such as transcription factor(s) regulated by GATA-1 activate the KLF13 gene promoter through the CCAAT or neighboring sequences. The former possibility may be supported by the evidence that the binding to CCAAT element is very unstable [17]. In addition, the non-canonical GATA-1 binding sequence, GATT that overlaps with the distal CCAAT motif of the KLF13 gene promoter (Fig. 4), is supposedly recognized by the GATA-1 carboxyl finger [18]. Therefore, the binding of GATA-1 to the promoter region in vivo may not necessarily be ruled out, even though we failed to demonstrate it in vitro. It should also be mentioned that a number of factors including CP1/NF-Y and CP2 which are expressed in a wide variety of tissues interact with the CCAAT motif [19]. It is therefore possible that GATA-1 activates KLF13 through enhancements of expression of such ubiquitously expressed factors. GATA-1 is also known to influence the expression of other erythroid transcription factors, e.g. EKLF [20], KLFD [21] and GATA-1 itself [22,23]. It has been shown that NF-E4 is a co-factor of CP2 [24], a transcription factor abundantly expressed in erythroid cells and involved in γ globin gene regulation. It is conceivable that GATA-1 activates NF-E4 which may bind to the KLF13 CCAAT box through CP2 and enhance KLF13 expression. It remains to be, however, tested whether the expression of NF-E4 is under the control of GATA-1. The mechanism of action of GATA-1 on the KLF13 promoter remains therefore unknown.

Acknowledgments

This work was supported by NIH grant HL20899 (subcontract 225053).

References

[1] S. Philipsen, G. Suske, A tale of three fingers: the family of mammalian Sp/XKLF transcription factors, Nucleic Acids Res. 27 (1999) 2991–3000.
[2] J.J. Bieker, Krüppel-like factors: three fingers in many pies, J. Biol. Chem. 276 (2001) 34355–34358.
[3] J. Kaczynski, T. Cook, R. Urrutia, Sp1- and Krüppel-like transcription factors, Genome Biol. 4 (2003) 206.
[4] I.J. Miller, J.J. Bieker, A novel, erythroid cell-specific murine transcription factor that binds to the CACCC element and is related to the Krüppel family of nuclear proteins, Mol. Cell. Biol. 13 (1993) 2776–2786.
[5] B. Nuez, D. Michalovich, A. Bygrave, R. Ploemacher, F. Grosveld, Defective haematopoiesis in fetal liver resulting from inactivation of the EKLF gene, Nature 375 (1995) 316–318.
[6] A.C. Perkins, A.H. Sharpe, S.H. Orkin, Lethal β-thalassaemia in mice lacking the erythroid CACCC-transcription factor EKLF, Nature 375 (1995) 318–322.
[7] D. Donze, T.M. Townes, J.J. Bieker, Role of erythroid Kruppel-like factor in human γ- to β-globin gene switching, J. Biol. Chem. 270 (1995) 1955–1959.

[8] H. Asano, G. Stamatoyannopoulos, Activation of β-globin promoter by erythroid Krüppel-like factor, Mol. Cell. Biol. 18 (1998) 102–109.
[9] K.P. Anderson, C.B. Kern, S.C. Crable, J.B. Lingrel, Isolation of a gene encoding a functional zinc finger protein homologous to erythroid Krüppel-like factor: identification of a new multigene family, Mol. Cell. Biol. 15 (1995) 5957–5965.
[10] M.A. Wani, S.E. Wert, J.B. Lingrel, Lung Krüppel-like factor, a zinc finger transcription factor, is essential for normal lung development, J. Biol. Chem. 274 (1999) 21180–21185.
[11] H. Asano, X.S. Li, G. Stamatoyannopoulos, FKLF-2: a novel Krüppel-like transcriptional factor that activates globin and other erythroid lineage genes, Blood 95 (2000) 3578–3584.
[12] A. Song, Y.F. Chen, K. Thamatrakoln, T.A. Storm, A.M. Krensky, Transcriptional regulation of RANTES expression in T lymphocytes, Immunity 10 (1999) 93–103.
[13] K.M. Martin, W.N. Cooper, J.C. Metcalfe, P.R. Kemp, Mouse BTEB3, a new member of the basic transcription element binding protein (BTEB) family, activates expression from GC-rich minimal promoter regions, Biochem. J. 345 (2000) 529–533.
[14] H. Asano, X.S. Li, G. Stamatoyannopoulos, FKLF, a novel Krüppel-like factor that activates human embryonic and fetal β-like globin genes, Mol. Cell. Biol. 19 (1999) 3571–3579.
[15] J. Sambrook, D.W. Russell, Molecular Cloning: A Laboratory Manual, 3rd ed., Cold Spring Harbor Laboratory Press, New York, 2001.
[16] M. Berry, F. Grosveld, N. Dillon, A single point mutation is the cause of the Greek form of hereditary persistence of fetal haemoglobin, Nature 358 (1992) 499–502.
[17] Q. Li, Z.J. Duan, G. Stamatoyannopoulos, Analysis of the mechanism of action of non-deletion hereditary persistence of fetal hemoglobin mutants in transgenic mice, EMBO J. 20 (2001) 157–164.
[18] D.J. Whyatt, E. deBoer, F. Grosveld, The two zinc finger-like domains of GATA-1 have different DNA binding specificities, EMBO J. 12 (1993) 4993–5005.
[19] R. Mantovani, The molecular biology of the CCAAT-binding factor NF-Y, Gene 239 (1999) 15–27.
[20] M. Crossley, A.P. Tsang, J.J. Bieker, S.H. Orkin, Regulation of the erythroid Krüppel-like factor (EKLF) gene promoter by the erythroid transcription factor GATA-1, J. Biol. Chem. 269 (1994) 15440–15444.
[21] A.C. Oates, S.J. Pratt, B. Vail, Y. Yan, R.K. Ho, S.L. Johnson, J.H. Postlethwait, L.I. Zon, The zebrafish klf gene family, Blood 98 (2001) 1792–1801.
[22] S.F. Tsai, E. Strauss, S.H. Orkin, Functional analysis and in vivo footprinting implicate the erythroid transcription factor GATA-1 as a positive regulator of its own promoter, Genes Dev. 5 (1991) 919–931.
[23] K. Nishikawa, M. Kobayashi, A. Masumi, S.E. Lyons, B.M. Weinstein, P.P. Liu, M. Yamamoto, Self-association of gata1 enhances transcriptional activity in vivo in zebra fish embryos, Mol. Cell. Biol. 23 (2003) 8295–8305.
[24] W. Zhou, D.R. Clouston, X. Wang, L. Cerruti, J.M. Cunningham, S.M. Jane, Induction of human fetal globin gene expression by a novel erythroid factor, NF-E4, Mol. Cell. Biol. 20 (2000) 7662–7672.

Leukemia (2005) 19, 674–684

www.nature.com/leu

CORRESPONDENCE

Increased erythropoietin level and reticulocyte count during arsenic trioxide therapy

Leukemia (2005) **19**, 674–676. doi:10.1038/sj.leu.2403635
Published online 3 February 2005

TO THE EDITOR

The efficacy of arsenic trioxide (ATO) in relapsed patients with acute promyelocytic leukemia (APL) has been established. ATO can be used as a single agent and induces complete remission with only minimal myelosuppression. Several reports showed that 80–85% of relapsed APL patients achieved complete remission with ATO alone. The 18-month overall survival was 42–66%.[1,2]

The most important adverse event with ATO therapy is prolongation of the QT/QTc interval on ECG. This event was reportedly observed in 40–93% of ATO-administered patients and was occasionally accompanied with ventricular tachycardia including torsades de pointes.[3,4] In hematological toxicity, however, only leukocytosis during ATO-induction therapy was reported.[1,2] Furthermore, the effect of ATO therapy on normal hematopoiesis has not been carefully analyzed.

From 1999 to 2004, we experienced nine APL patients who had been treated with ATO as a phase II study of ATO therapy for relapsed APL patients at Nagoya University Hospital. All patients relapsed after ATRA and conventional chemotherapy. For induction therapy, treatment (0.15 mg/kg daily) was discontinued before day 60 if the patients had achieved bone marrow remission or if substantial toxicity was observed. Patients who had achieved complete remission were treated with subsequent two consolidation therapies (0.15 mg/kg daily

Table 1 Disease status of patients received ATO consolidation therapy

Case	*Age*	*Sex*	*Disease status (No. of CR)*	*Number of ATO consolidation*
1	62	M	5	6
2	31	M	4	2
3	30	M	2	2
4	41	M	2	2
5	63	M	4	2
6	34	F	2	1
7	53	F	2	2

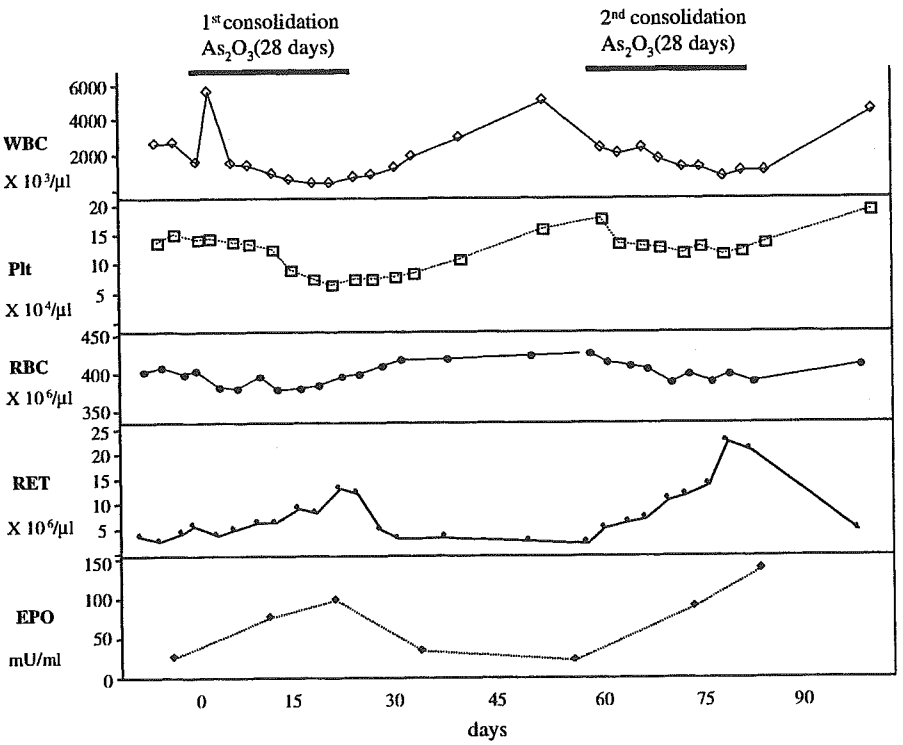

Figure 1 Clinical course of patient 4. Severe neutropenia and remarkable increase of reticulocyte and Epo were observed. Progression of anemia and thrombocytepenia were mild (ATO, arsenic trioxide; WBC, white blood cell; RBC, red blood cell; Plt, platelets; Ret, reticulocyte; Epo, erythropoietin).

Correspondence: Dr T Kajiguchi, Department of Hematology, Graduate School of Medicine, Nagoya University, 65 Tsurumai-cho, Showa-ku, Nagoya 466-8550, Japan; Fax: +81-52-744-2161;
E-mail: tomokaji@abox3.so-net.ne.jp
Received 31 October 2004; accepted 17 November 2004; Published online 3 February 2005

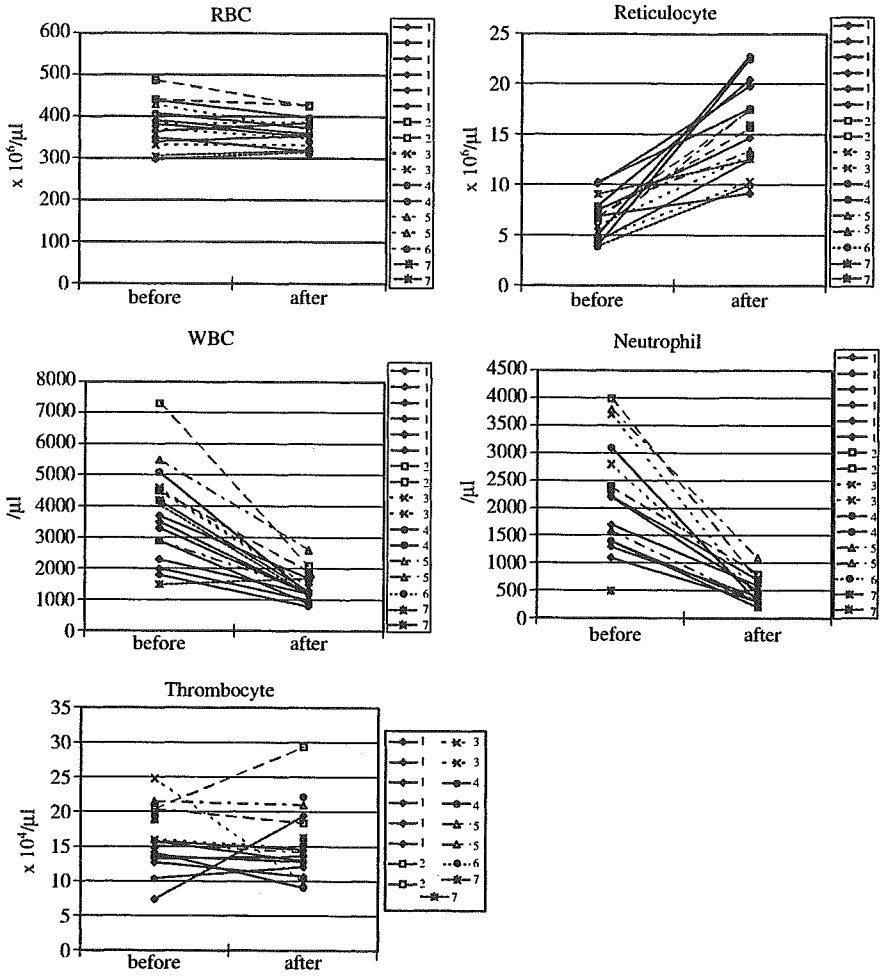

Figure 2 CBC data during ATO consolidation therapy. Reticulocyte increased in all 17 course of ATO consolidation ($P<0.0001$). WBC and neutrophil remarkably decreased after the therapy ($P<0.0001$). RBC slightly decreased ($P=0.011$) and thrombocyte showed little change during the therapy ($P=0.62$). *P*-values were calculated by paired *T*-test.

for 28 days) after 3–6-week intervals. Eight achieved complete remission and seven had consolidation therapy with ATO. In seven patients, only case 1, as PML-RARα was positive by RT-PCR after the second course of consolidation therapy, received four more courses of ATO consolidation therapy (shown in Table 1).

A typical clinical course is shown in Figure 1. Although the white blood cell (WBC) count decreased during ATO consolidation therapy, little change was observed in red blood cell (RBC). The reticulocyte count increased during ATO consolidation therapy, and without the therapy, it decreased to the normal range. Similar to reticulocytes, the serum erythropoietin (Epo) concentration increased during the treatment and then decreased. During therapy, no signs of hemolysis such as erythrocyte destruction, decreased haptoglobin, increased indirect bilirubin and LDH were observed.

The CBC data in 17 courses of ATO consolidation are shown in Figure 2. The examinations were performed 1 or 2 days before ATO consolidation (before) and on the last day or the day before the last day of ATO consolidation (after). After ATO treatment, reticulocytes increased in all seven patients ($P<0.0001$). In addition, the serum concentration of Epo also increased in all 7 patients, in 10 courses examined (shown in Figure 3a, $P=0.0024$). These data suggest that the increase of reticulocytes depends on the increase of Epo concentration. On the other hand, WBC and neutrophils remarkably decreased after therapy ($P<0.0001$). RBC slightly decreased during therapy ($P=0.011$); increased with five courses in three patients and decreased with 12 courses in seven patients. Reticulocytes increased in both groups (increased: $P=0.046$; decreased: $P<0.0001$). Thrombocytes showed little change during therapy ($P=0.62$).

These clinical findings suggest that ATO can induce the expression of Epo. To study this mechanism, we used a human hepatoma cell line, Hep3B, in which Epo production is markedly increased after exposure to hypoxia or cobalt chloride ($CoCl_2$).[5] We investigated the effect of ATO on the mRNA expression of Epo in Hep3B cells using real-time PCR examination. In an atmosphere of 20% O_2, the expression of Epo mRNA increased up to seven times in a therapeutic concentration (0.5 μM) of ATO treatment for 24 h. On the other hand, with a higher concentration (2.5 μM) of ATO, cell growth was inhibited at this concentration, and the expression of Epo decreased to the baseline (Figure 3b). These findings suggest that Epo is directly induced by ATO in APL patients.

Using Hep3B and HepG2 cell lines, it was reported that expression of Epo regulated by a major transcriptional factor, hypoxia inducible factor 1, HIF-1.[6,7] HIF-1 is a basic helix-loop-helix transcription factor, composed of two subunits, HIF-1α and HIF-1β HIF-1β is constitutively expressed, whereas HIF-1α expression is increased upon hypoxia or in response to $CoCl_2$.

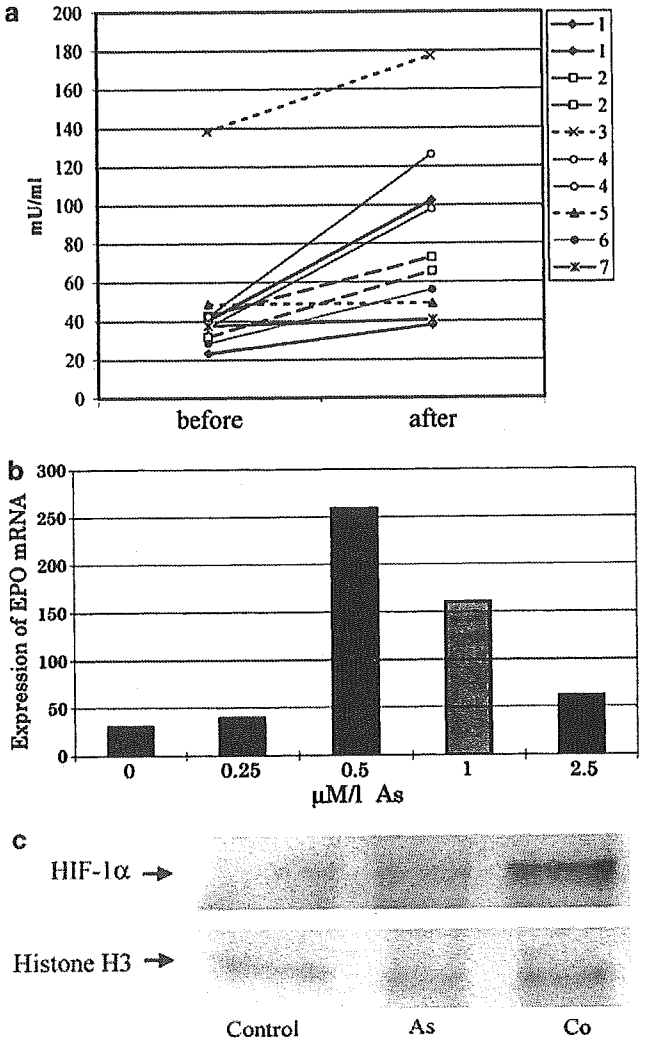

Figure 3 Serum concentration of Epo in the patients with ATO consolidation therapy (a). The concentration of Epo was measured using a radioimmune assay in the SRL laboratory (Tachikawa, Japan). The serum concentration of Epo increased in all patients and in all courses examined ($P=0.0024$). Epo mRNA expression level in Hep3B cell line using RQ-PCR (b). Total RNA was obtained from Hep3B cells which were treated with or without ATO and hypoxia (1% O_2) using RNA STAT-60 (Tel-Test Inc., Friendswood, TX, USA). One microgram of total RNA was transcribed into cDNA using MuLV-reverse transcriptase (Applied Biosystems, Foster city, CA, USA) at 42°C for 1 h in a total volume of 40 μl containing 0.1 nmol Random Hexamers (Applied Biosystems), 1 mM of each dNTP, 100 U of MuLV-reverse transcriptase (Applied Biosystems), 40 U of RNase Inhibitor, 1 × buffer (50 mM Tris-HCl, pH 8.3, 50 mM KCl, 5 mM $MgCl_2$). At the end of incubation, the reaction mixture was heated to 70°C for 10 min. The expression level of Epo transcript was quantified by a real-time fluorescence detection method on an ABI Prism 7000 sequence detection system using Assays-on-Demand Gene Expression products (Applied Biosystems). The housekeeping gene, GAPDH, was used as a control for cDNA quality. Relative gene expression levels were calculated using standard curves and adjusted based on the expression level of the GAPDH gene. Each gene expression level was analyzed in triplicate and the mean was subjected to analysis. Western blotting analysis for HIF-1α in Hep3B cell line (c). In all, 20 μg of nuclear extracts from Hep3B cells were used for each lane. Upper panel indicates HIF-1α protein expression. Lower panel shows histone H3 as a loading control. A representative result of three independent experiments with consistent results is shown (Cont, no treat; ATO, the cells were treated with 0.5 μM ATO for 24 h; Co, the cells were treated with 100 μM $CoCl_2$ for 1 h).

In normoxia, HIF-1α is rapidly ubiquitinated by the von hippel-lindau tumor suppressor E3 ligase complex and subjected to proteasomal degradation. Under hypoxic conditions, the degradation of HIF-1α is suppressed, and accumulates to form an active complex with HIF-1β. This activated HIF-1 complex binds at the Epo enhancer, resulted in increase of Epo expression.[6] We therefore investigated the protein level of HIF-1α by Western blotting analysis. As shown in Figure 3c, a remarkable increase of HIF-1α protein was detected in $CoCl_2$-treated Hep3B, and a moderate increase of HIF-1α protein was detected in ATO-treated Hep3B. These results suggest that ATO increased protein level of HIF-1α resulting in Epo expression in Hep3B cells. Some reports showed that the Epo gene is negatively regulated under normoxic conditions by GATA-2, which binds to the GATA site of the Epo promoter in Hep3B cells.[8] We investigated the expression of GATA-2 in Hep3B, but no difference was observed between ATO-treated and non-treated Hep3B (data not shown). These results suggest that ATO increases Epo expression by modulating the expression of HIF-1α.

While RBC increased with five courses in three patients and decreased with 12 courses in seven patients, the reticulocyte count increased in all courses. These results suggest that the increase of reticulocytes during therapy is a reaction to the increase of Epo concentration but not to anemia. Despite the increased Epo and reticulocytes, polycythemia was not observed in patients with ATO. In bone marrow, erythroblasts increased and megaroblastic change was often observed (date not shown). No evidence of hemolysis and blood loss was detected in these patients. These results suggest that dyserythropoiesis may also exist in ATO-treated patients. Further studies should be performed to clarify the details of erythropoiesis in ATO-treated patients.

T Kajiguchi[1]
K Yamamoto[1]
M Sawa[1]
N Emi[1]
T Naoe[1]

[1]*Department of Hematology, Graduate School of Medicine, Nagoya University, Showa-ku, Nagoya, Japan*

References

1 Soignet SL, Frankel SR, Douer D, Tallman MS, Kantarjian H, Calleja E *et al.* United States multicenter study of arsenic trioxide in relapsed acute promyelocytic leukemia. *J Clin Oncol* 2001; **19**: 3852–3860.
2 Ohnishi K, Yoshida H, Shigeno K, Nakamura S, Fujisawa S, Naito K *et al.* Arsenic trioxide therapy for relapsed or refractory Japanese patients with acute promyelocytic leukemia: need for careful electrocardiogram monitoring. *Leukemia* 2002; **16**: 617–622.
3 Unnikrishnan D, Dutcher JP, Varshneya N, Lucariello R, Api M, Garl S *et al.* Torsades de pointes in 3 patients with leukemia treated with arsenic trioxide. *Blood* 2001; **97**: 1514–1516.
4 Ohnishi K, Yoshida H, Shigeno K, Nakamura S, Fujisawa S, Naito K *et al.* Prolongation of the QT interval and ventricular tachycardia in patients treated with arsenic trioxide for acute promyelocytic leukemia. *Ann Intern Med* 2000; **133**: 881–885.
5 Goldberg MA, Glass GA, Cunningham JM, Bunn HF. The regulated expression of erythropoietin by two human hepatoma cell lines. *Proc Natl Acad Sci USA* 1987; **84**: 7972–7976.
6 Ebert BL, Bunn HF. Regulation of the erythropoietin gene. *Blood* 1999; **94**: 1864–1877.
7 Semenza GL, Nejfelt MK, Chi SM, Antonarakis SE. Hypoxia-inducible nuclear factors bind to an enhancer element located 3' to the human erythropoietin gene. *Proc Natl Acad Sci USA* 1991; **88**: 5680–5684.
8 Imagawa S, Yamamoto M, Miura Y. Negative regulation of the erythropoietin gene expression by the GATA transcription factors. *Blood* 1997; **89**: 1430–1439.

lies of Asian and Western European ancestry. Blood 2003; 102:1097-9.
8. Pastore Y, Jedlickova K, Guan Y, Liu E, Fahner J, Hasle H, et al. Mutations of von Hippel-Lindau tumor-suppressor gene and congenital polycythemia. Am J Hum Genet 2003;73:412-9.
9. Cario H, Schwarz K, Jorch N, Kyank U, Petrides PE, Schneider DT, et al. Mutations in the von Hippel-Lindau (VHL) tumor suppressor gene and VHL-haplotype analysis in patients with presumable congenital erythrocytosis. Haematologica 2005; 90:19-24.
10. Bento MC, Ko-Tung C, Guan Y, Liu E, Caldas G, Gatti RA, et al. Congenital polycythemia with homozygous mutations of von Hippel-Lindau gene: five new Caucasian patients. Haematologica 2005;90:128-9.

Myelodysplastic Syndromes

Lack of mutations of the human telomerase RNA gene (hTERC) in myelodysplastic syndrome

Myelodysplastic syndrome (MDS), considered a pre-leukemic state, has recently been categorized as a subset of bone marrow failure syndromes. Unlike other subtypes of bone marrow failure syndromes, such as aplastic anemia or dyskeratosis congenita,[1] little is known about genetic alterations of human telomerase in MDS, despite the fact that immune cells from patients with MDS frequently exhibit telomere attrition.

haematologica 2005; 90:691
(http://www.haematologica.org/journal/2005/5/691.html)

Human telomerase RNA (hTERC) is an essential component of the telomerase ribonucleoprotein complex, and mutations in hTERC can result in haploid insufficiency, reducing telomerase activity,[2] leading to premature telomere shortening. Identification of mutations of hTERC in bone marrow failure syndromes, including myelodysplastic syndrome (MDS), may provide insights into the underlying molecular causes of these syndromes.

In the present study, we investigated mutations of the hTERC gene (*NT 005612.14*) using polymerase chain reaction-direct sequencing in 42 marrow samples from 35 consecutive MDS patients (34 to 80 years old); 19 had refractory anemia (RA), 14 had RA with excess blasts (RAEB), and two patients had RAEB in transformation. Seven RAEB patients were also studied at the time their disease transformed into acute myeloid leukemia. Blood samples were also obtained from 134 healthy volunteers (4 to 90 years old). All samples were collected from Japanese patients and healthy volunteers after obtaining informed consent. Telomere length and telomerase activity were measured as previously described in mononuclear cells.[3]

We selected seven hTERC loci; C98T, the template region G58A, pseudoknot domain C72T and Δ110-113, CR4-CD5 domain G305A and G322A, and Box H/ACA domain G450A, to identify possible mutations of the hTERC gene. We also examined polymorphisms at 514. Direct sequencing showed no heterozygous hTERC mutations of these loci in 42 MDS samples and 134 healthy volunteers, although MDS patients had variable telomere lengths (short in 27%, normal in 69%, and long in 5% compared to normal volunteers) with low telomerase activity. We did not find allelic variations at the 514 locus in healthy populations: AA genotype (MDS 11.1% versus control 11.9%), AG genotype (MDS 55.6% versus control 51.4%), and GG genotype (MDS 33.3% versus control 36.7%) and no deviation was notable in MDS patients. hTERC mutations at certain loci affect telomerase activity, and most MDS patients show normal to low levels of telomerase activity; nevertheless, cells from some MDS patients have telomere attrition. In one study it was reported that, out of 55 MDS patients, two black patients had a G58A change and one other patient had a G322A substitution.[4] More recently a black MDS patient with G58A was also reported.[5] Since the G58A substitution seems to be common in the black population (5/24 normal subjects)[5] and no G58A mutations in the hTERC gene were detected among the normal Japanese population or in the MDS patients in our study, mutations in the hTERC gene are unlikely to be related to telomere changes observed in most MDS patients. Since some MDS patients have shortened telomeres and also low telomerase activity, it remains possible that the dysfunction of telomere regulation in MDS patients may be caused by alterations in other proteins that interact with telomerase or in the catalytic component (hTERT) itself.

Kazuma Ohyashiki, Jerry W. Shay,° Junko H. Ohyashiki#*

**First Department of Internal Medicine, Tokyo Medical University, Tokyo, Japan; °Department of Cell Biology, University of Texas Southwestern Medical Center at Dallas, TX, USA; #Intractable Immune System Disease Research Center, Tokyo Medical University, Tokyo, Japan*

Key words: telomerase, hTERC mutations, myelodysplastic syndrome.

Correspondence: Kazuma Ohyashiki, M.D., First Department of Internal Medicine (Hematology/Oncology division), Tokyo Medical University, 6-7-1 Nishi-shinjuku, Shinjuku-ku, Tokyo 160-0023, Japan. Phone: international +81.3.33422520. Fax: international +81.3-53816651. E-mail: ohyashik@rr.iij4u.or.jp

References

1. Fogarty PF, Yamaguchi H, Wiestner A, Baerlocher GM, Sloand E, Zeng WS, et al. Late presentation of dyskeratosis congenita as apparently acquired aplastic anaemia due to mutations in telomerase RNA. Lancet 2003;362:1628-30.
2. Ly H, Blackburn EH, Parslow TG. Comprehensive structure-function analysis of the core domain of human telomerase RNA. Mol Cell Biol 2003;23:6849-56.
3. Iwama H, Ohyashiki K, Ohyashiki JH, Hayashi S, Yahata N, Ando K, et al. Telomeric length and telomerase activity vary with age in peripheral blood cells obtained from normal individuals. Hum Genet 1998;102:397-402.
4. Yamaguchi H, Baerlocher GM, Lansdorp PM, Chanock SJ, Nunez O, Sloand E, et al. Mutations of the human telomerase RNA gene (TERC) in aplastic anemia and myelodysplastic syndrome. Blood 2003;102:916-8.
5. Wilson DB, Ivanovich J, Whelan A, Goodfellow PJ, Bessler M. Human telomerase RNA mutations and bone marrow failure. Lancet 2003;361:1993-4.

Myelodysplastic Syndromes

Secondary myelodysplastic syndromes following treatment with azathioprine are associated with aberrations of chromosome 7

We report 14 cases of secondary myelodysplastic syndromes (sMDS) following treatment with azathioprine for non-malignant disorders. Long-term treatment with azathioprine seems to be associated with an increased risk of MDS and subsequent leukemic transformation.

haematologica 2005; 90:691-693
http://www.haematologica.org/journal/2005/5/691a.html)

The JAK2 V617F tyrosine kinase mutation in myelodysplastic syndromes (MDS) developing myelofibrosis indicates the myeloproliferative nature in a subset of MDS patients

Leukemia (2005) **19**, 2359–2360. doi:10.1038/sj.leu.2403989; published online 20 October 2005

TO THE EDITOR

The JAK2 V617F tyrosine kinase mutation is responsible for the development of *BCR/ABL*-negative chronic myeloproliferative disorders, including myelofibrosis (MF).[1–4] Kralovics *et al*[1] demonstrated that 74% of patients with polycythemia vera (PV), 32% of essential thrombocythemia (ET), and 35% of patients with primary MF harbored the JAK2 V617F mutation. Recently, Steensma *et al*[5] demonstrated that 5% (five of 101 patients) of myelodysplastic syndromes (MDS) patients had the JAK2 V617F tyrosine kinase mutation and reported its infrequent occurrence in other myeloid disorders, including MDS. However, the exact significance of the JAK2 V617F mutation in MDS is obscure. Myelofibrosis is associated with various hematologic diseases as a terminal hematologic condition and is an important issue in managing patients. Less than 10% of myelodysplastic syndromes (MDS) develop MF during their courses and most of them have unfavorable prognoses.[6] The exact biology of MF in MDS patients is still unknown, since some MDS patients show aspects of both MDS and myeloproliferative disorders,[7] and therefore, it is possible that MF could be associated with MDS as one phenotype of myelproliferative disorders.

We therefore searched for the JAK2 V617F mutation in primary and secondary MF in various hematologic diseases using frozen marrow cells or peripheral blood mononuclear cells from patients after obtaining their written informed consent, using the sequence-specific primer-single molecule fluorescence detection assay (SSP-SMFD) (Bannai M, Higuchi K, Akesaka T, Furukawa M, Yamaoka M, Sato K, Tokunaga K. Single-nucleotide-polymorphism genotyping for whole-genome-amplified samples using automated fluorescence correlation spectroscopy. *Annal Biochem* 2004; **327**: 215–221). We adopted G→T mutation when the incidence of T-substitute reached more than 10%. Furthermore, we also confirmed the JAK2 V617F mutation using a PCR direct-sequencing (Figure 1).

Of the MF patients associated with acute myeloid leukemia ($n=3$), lymphoma ($n=3$), and chronic myeloid leukemia ($n=3$), none showed the mutation at the time of diagnosis of MF. Approximately 40% of ET (seven of 16 patients) and primary MF (one of four patients) showed the JAK2 V617F mutation, whereas six of eight patients (75%) with PV showed the mutation. Of note is that two of six patients with MDS terminating in MF showed the mutation at the time of MF, while no MDS patient without MF (MDS: $n=38$: 20 had refractory anemia (RA), 16 had RA excess blasts (RAEB), and two patients had RAEB in transformation) had the JAK2 V617F mutation (Figure 1). Our study demonstrated that MDS with MF is sometimes associated with the JAK2 V617F mutation, while other underlying diseases developing MF may involve other pathways. Moreover, these findings permit speculation that MDS patients with the JAK2 V617F mutation may be responsible for secondary MF in MDS patients during the process of MDS progression. Another possibility is that the JAK2 V617F mutation

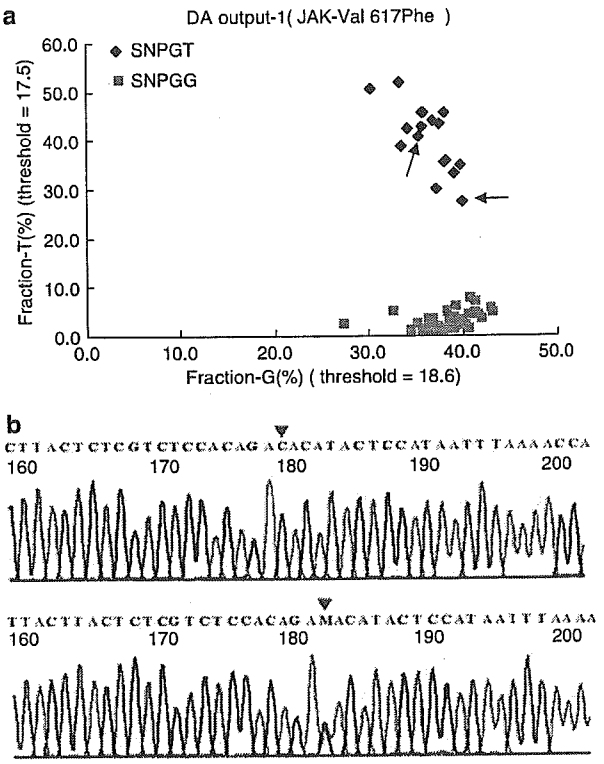

Figure 1 We assessed the JAK2 V617F mutation by the sequence-specific primer single-molecule fluorescence detection assay (SSP-SMFD) (Bannai M, Higuchi K, Akesaka T, Furukawa M, Yamaoka M, Sato K, Tokunaga K. Single-nucleotide-polymorphism gonotyping for whole-genome-amplified samples using automated fluorescence correlation spectroscopy. *Annal Biochem* 2004; **327**: 215–221). This technique utilizes primer extension technology combined with fluorescent polarization. In this method, a fluorescent-labeled ddNTP specific for the mutation is incorporated into the primer, which binds immediately upstream from the mutation site, and the difference in fluorescent polarization between incorporated and unincorporated dd NTPs is detected. Percentages (horizontal axis (G) and vertical axis (T)) indicate extension efficacy of the 20 nm primer, and we adopted G→T mutation when the incidence of T-substitute reached ⩾10%. Diamonds indicate patients with deviation of G→T substitute corresponding to the JAK2 V617F mutation (a). Arrows indicate patients with MDS with MF. PCR-direct sequencing of the complementary strand was also performed in order to confirm mutation of the JAK2 V617F tyrosine kinase (NM_004972) in patients with myelodysplastic syndrome with myelofibrosis. The PCR conditions were as follows; preheating at 95°C for 10 min, followed by 40 cycles at 95°C for 30 s, 64°C for 30 s, and 72°C for 1 min, and a final extension at 72°C for 10 min. Reactions for direct sequencing of the PCR product were performed with BigDye Terminator ver3.1 (Perkin-Elmer Cetus, Fremont, CA, USA). The upper panel shows no mutation of the JAK2 V617F mutation, and the lower panel shows the C→A substitution of the complementary reverse strand, resulting in the JAK2 V617F mutation (G→T substitution in the forward strand). M indicates C→A mutation of the complementary reverse strand (b).

Correspondence: Dr K Ohyashiki, First Department of Internal Medicine, Tokyo Medical University, 6-7-1 Nishi-shinjuku, Shinjuku-ku, Tokyo 160-0023, Japan; Fax: +81 3 5381 6651;
E-mail: ohyashik@rr.iij4u.or.jp
Received 18 August 2005; accepted 9 September 2005; published online 20 October 2005

may previously exist and its clinical manifestation mimics MDS, that is, myelodysplastic features with cytopenias, but its biologic nature is closely associated with myeloproliferative disorders. Unfortunately, we did not detect its mutation before MF in our MDS/MF patients. Although MDS patients with MF have an unfavorable prognosis, the current study demonstrates the genotypic heterogeneity of such patients.

Acknowledgements

Thanks are due to Professor J Patrick Barron for his review of this manuscript and Mr Kunio Hori and Tohru Makino, NovusGene, Tokyo, for their technical assistance. This work was supported in part by a Grant-in-Aid for 'Intractable Hematopoietic Diseases' from the Ministry of Health, Welfare, and Labor, Japan (to KO), the 'High-Tech Research Center' Project from the Ministry of Education, Culture, Sports, Science and Technology: MEXT) (to KO, JHO), and by the 'University-Industry Joint Research Project' from MEXT (to KO, JHO).

K Ohyashiki[1]
Y Aota[1]
D Akahane[1]
A Gotoh[1]
K Miyazawa[1]
Y Kimura[1]
JH Ohyashiki[2]

[1]*The First Department of Internal Medicine, Tokyo Medical University, Tokyo, Japan; and* [2]*Intractable Immune System Research Center, Tokyo Medical University, Tokyo, Japan*

References

1 Kralovics R, Passamonti F, Buser AS, Teo SS, Tiedt R, Passweg JR *et al.* A gain-of-function mutation of Jak2 in myeloproliferative disorders. *N Engl J Med* 2005; **352**: 1779–1790.
2 Levine RL, Wadleigh M, Cools J, Ebert BL, Wernig G, Huntly BJ *et al.* Activating mutation in the tyrosine kinase JAK2 in polycythemia vera, essential thrombocythemia, and agnogenic myeloid metaplasia. *Cancer Cell* 2005; **7**: 387–397.
3 James C, Ugo V, Le Couedic JP, Staerk J, Delhommeau F, Lacout C *et al.* A unique clonal JAK2 mutation leading to constitutive signalling causes polycythaemia vera. *Nature* 2005; **484**: 1144–1148.
4 Baxter EJ, Scott LM, Campbell PJ, East C, Fourouclas N, Swanton S *et al.* Cancer genome project. Acquired mutation of the tyrosine kinase JAK2 in human myeloproliferative disorders. *Lancet* 2005; **365**: 1054–1061.
5 Steensma DP, Dewald GW, Lasho TL, Powell HL, McClure RF, Levine RL *et al.* The JAK2 V617F activating tyrosine kinase mutation is an infrequent event in both 'atypical' myeloproliferaive disorders and myelodysplastic syndromes. *Blood* 2005; **106**: 1207–1209.
6 Ohyashiki K, Sasao I, Ohyashiki JH, Murakami T, Iwabuchi A, Tauchi T *et al.* Clinical and cytogenetic characteristics of myelodysplastic syndromes developing myelofibrosis. *Cancer* 1991; **68**: 178–183.
7 Ohyashiki K, Yokoyama K, Kimura Y, Ohyashiki JH, Ito Y, Kuratsuji T *et al.* Myelodysplastic syndrome evolving into a myeloproliferative disorder: one disease or two? *Leukemia* 1993; **7**: 338–340.

Angiogenesis and mast cells in Hodgkin lymphoma

Leukemia (2005) **19**, 2360–2362. doi:10.1038/sj.leu.2403992; published online 13 October 2005

TO THE EDITOR

Hodgkin lymphoma (HL) differs from other lymphomas because the malignant cells, the Hodgkin and Reed–Sternberg (HRS) cells, are in minority and the majority of the tissue consists of surrounding benign cells, for example, eosinophilic granulocytes and mast cells, fibrosis and a varying number of microvessels. It has recently been reported that angiogenesis correlates to poor prognosis in HL.[1]

We have previously reported that HL patients with many mast cells in their tumour tissue have a worse prognosis.[2] Mast cells produce functionally active CD30 ligand (CD30L) and the poorer prognosis has been proposed to be caused by a stimulation of HRS by CD30L.[3] Furthermore, we have shown that mast cells, upon stimulation with CD30, release cytokines and chemokines, among which interleukin-8 (IL-8) is known to have angiogenic properties (manuscript in preparation). In other lymphomas, mast cells are proposed to contribute to angiogenesis.[4]

In order to increase our understanding of inflammatory cells, their importance in tumour progression and especially angiogenesis in HL, we investigated the possible relation between the number of mast cells and the microvessel count in primary diagnostic HL tissue. We also wanted to further elucidate the prognostic implication of microvessel count in HL.

Patient samples and clinical data were acquired from the database of the National Health Care Programme for HL in Sweden. A total of 120 patients treated with curative intention, according to the principles of the Health Care Programme[2] in the Uppsala/Örebro health care region between 1989 and 1994, were included. The paraffin-embedded tissue samples were from HL involved lymph nodes from the primary diagnosis. The clinical characteristics are presented in Table 1. Progression free survival (PFS) and HL specific survival (HLS) were analysed. The mean follow-up of living patients was 11 years (range 6–15 years).

The estimation of the number of microvessels immunohistochemically stained for CD31 (Figure 1), was done by one of the authors using the Chalkley technique.[5] Three to five fields with the highest concentration of vessels (a hot spot) were counted and an average of the highest three countings in every case was used. In all, 20 cases were recounted independently by another author and the counts correlated with an R-value of 0.75, ($P=0.0002$). All evaluations were done without knowledge of patient data. The counts varied from 1 to 12 vessels/hot spot. The median was 3 and the 75th percentile was 4.3 vessels/hot spot. Nonbulky disease correlated to high microvessel count (Table 1) and there was a lower proportion of patients with WBC>15 in the upper quartile group (data not shown), but there were no other correlations to histology, laboratory parameters, stage, B-symptoms or sex.

In univariate analyses, HL patients with a high microvessel count, cutoff at the 75th percentile ($n=33$), have a worse PFS

Correspondence: Dr I Glimelius, Department of Oncology, Radiology and Clinical Immunology, Uppsala University Hospital, Rudbeck laboratory C11, Uppsala S-751 85, Sweden; Fax: +46 18 611 34 32; E-mail: Ingrid.Glimelius@home.se
Received 30 August 2005; accepted 15 September 2005; published online 13 October 2005